Energy Harvesting Applications of Ionic Polymers

by

Benjamin R. Martin

Thesis submitted to the Faculty of the
Virginia Polytechnic Institute and State University
in partial fulfillment of the requirements for the degree of

Master of Science

in

Mechanical Engineering

Donald J. Leo, Chair
Daniel J. Inman
Harry H. Robertshaw

April, 22 2005
Blacksburg, Virginia

Keywords: Ionic Polymers, Energy Harvesting, Energy Scavenging, Energy Storage

Energy Harvesting Applications of Ionic Polymers

Benjamin R. Martin

Abstract

The purpose of this thesis is the development and analysis of applications for ionic polymers as energy harvesting devices. The specific need is a self-contained energy harvester to supply renewable power harvested from ambient vibrations to a wireless sensor. Ionic polymers were investigated as mechanical to electrical energy transducers. An ionic polymer device was designed to harvest energy from vibrations and supply power for a wireless structural health monitoring sensor.

The ionic polymer energy harvester is tested to ascertain whether the idea is feasible. Transfer functions are constructed for both the open-circuit voltage and the closed-circuit current. The impedance of the device is also quantified. Using the voltage transfer function and the current transfer function it is possible to calculate the power being produced by the device.

Power generation is not the only energy harvesting application of ionic polymers, energy storage is another possibility. The ionic polymer device is tested to characterize its charge and discharge capabilities. It is charged with both DC and AC currents. An energy storage comparison is performed between the ionic polymers and capacitors. While the polymers performed well, the electrolytic capacitors are able to store more energy. However, the ionic polymers show potential as capacitors and have the possibility of improved performance as energy storage devices. Current is measured across resistive loads and the supplied power is calculated. Although the power is small, the ionic polymers are able to discharge energy across a load proving that they are capable of supplying power.

To Jennifer Michael,
for never letting me quit.

Acknowledgments

A great deal of thanks is owed to Dr. Donald J. Leo for his advice, encouragement, support, and commitment during my degree and research. I also want to thank Dr. Daniel J. Inman and Dr. Harry H. Robertshaw for their input on my research and their service as members of my advising committee.

Thanks goes to my parents for encouraging and supporting me through my graduate and undergraduate career. And thank you to the rest of my family and friends for providing welcomed breaks from studying. Finally I would like to thank everyone I worked with at CIMSS for the help they provided.

This research has been supported by CSA Engineering, Inc. through the Navy's SBIR program. Special thanks to Sean O'F.Fahey of CSA who I worked with during the beginning of the project.

Contents

List of Tables

List of Figures

Nomenclature

A -cross-sectional area

C -end-condition constant for buckling

C_a -capacitance of ionic polymers

$\frac{dv}{dt}$ -derivative of voltage or the rate of flow of voltage

E -elastic modulus

$E(\omega)$ -frequency dependent elastic modulus of harvester device (EM1)

F_{dir} -directional force

F_a -axial force

F_l -lateral force

$f(\omega)$ -frequency dependent force of harvester device (EM1)

I -area moment of inertia

I_x -area moment of inertia about the x-axis of the cross-sectional area

I_y -area moment of inertia about the y-axis of the cross-sectional area

I_1 -area moment of inertia for the first beam

I_2 -area moment of inertia for the second beam

$I(\omega)$ -closed-circuit current transfer function

i -current

$i(\omega)$ -frequency dependent current

$i_c(\omega)$ -closed-circuit current

$Im(Z(j\omega))$ -imaginary component of the impedance transfer function

j -imaginary component

k_d -stiffness of the two-post device

$k(\omega)$ -stiffness transfer function of harvester device (EM1)

l -total length

l_f -free length

$(l/\kappa)_1$ -tangent slenderness ratio

m_h -head mass

P -power

P_{cr} -critical buckling load

$P(\omega)$ -frequency dependent power

R -resistance

Rp -resistance of the ionic polymers

S -slenderness ratio

S_y -yield strength

t -thickness

$u(\omega)$ -frequency dependent displacement

$V(\omega)$ -open-circuit voltage transfer function

$v_o(\omega)$ -open-circuit voltage

v -voltage

$v(\omega)$ -frequency dependent voltage

w -width

x -position on beam

x_{fit} -independent variable for discharging models

y_l -dependent variable for linear function discharging model

y_p -dependent variable for power function discharging model

$Z(\omega)$ -impedance transfer function

α_{dir} -directional acceleration

α_a -axial acceleration

β_n -weighted natural frequencies

δ -deflection

ϵ -strain

ϵ_a -axial strain

κ -radius of gyration

π -pi

ρ -density

σ_a -axial stress

σ_l -lateral stress

σ_n -mode shape coefficients

ω_n -natural frequency

Chapter 1

Introduction

1.1 Motivation

Energy harvesting or energy scavenging has become an area of increasing interest for researchers (Anonymous, 2003). Producing sustainable power sources from existing environmental conditions has many applications. One application that is being heavily pursued is using scavenged energy to power remote wireless sensors (Chandrakasan et al., 1999). Wireless sensors can be placed in locations and environments that have previously been unaccessible because of hard-wiring issues. In the case of micro electromechanical systems (MEMS), the size of the device and the fact that they can be wireless opens many possibilities where before a sensor or the wiring was too obtrusive. A main area of use for remote wireless sensors is structural health monitoring, the act of monitoring a structure and detecting damage at the earliest occurrence. Self-powered wireless sensors for structural health monitoring is the application driving the research presented here.

The specific application is for a small self-contained energy harvesting device mounted on the propulsors of a ship. The device will harvest energy from the vibrations of the propeller to support a wireless sensors or network of sensors that can monitor the propeller and propeller shaft. Ambient vibrations have already proven to be a viable energy source for wireless sensors (Roundy et al., 2003). It is important that the device be small and self-contained so that it does not disrupt the performance of the propeller or be damaged by the environmental conditions. Conditions could be hazardous as radial accelerations from the dynamics of the propeller are estimated to be on the order of 100 Gs. The reason for wanting a wireless self-powered design is that it will be more robust than a design that

relies on an external power source. Wiring and the mechanical parts associated with bringing external power to the propeller environment can fail. Therefore, using a well-designed device to harvest power from vibrations is more reliable and efficient.

Active materials have already been explored as mechanical to electrical energy transducers (Sodano et al., 2004). Ionic polymers offer several advantages as the choice of active material for the specific application. They have the potential for further development as electromechanical transducers since the technology is relatively new. Most work done with ionic polymers is research based, trying to model the behavior and either improve performance of realize it at lower costs. Also, ionic polymers can sustain large strains making them ideal for the high stress environment of the ship propulsors (Shahinpoor and Kim, 2001). The ability to endure large strains also allows the polymers to have a large stroke, which will be advantageous since operating frequencies are estimated to be between 0.2 and 4.2 Hz. These reasons make ionic polymers a perfect candidate to explore for energy harvesting applications in the described environment.

Ionic polymers have previously not been used for energy harvesting. This need provides a unique opportunity to explore a possible application of ionic polymer technology. It also provides an opportunity to characterize the mechanical to electrical production of the polymers and the energy storage capabilities.

1.2 Ionic Polymers

1.2.1 History

Research in active polymer materials has existed for over a century. The first experiments were conducted on rubber bands in 1880. However, the work that led to electroactive polymers (EAPs) did not occur until 1949 when chemically stimulated polymers were discovered and studied. The work with these chemomechanical polymers led directly to synthetic polymers that could be used for actuation. Before long electroactive polymers became prominent because of the convenience of the technology. Even with the increased interest in EAPs, the largest amount of work and progress only began in the 1990's (Bar-Cohen, 2001).

Ionic polymer-metal composites (IPMCs), a type of EAP, were originally developed as fuel cell membranes and not until the early 90's were their actuation and sensing properties discovered. The two properties were discovered concurrently, but by different re-

searchers. Sensing properties were discovered by Sadeghipoor in 1992, who was using them as hydrogen pressure transducers. The initial sensing use was as a vibration sensor. Also in 1992, Oguro described the actuation function of the IPMC's by bending them under applied voltages (Bar-Cohen, 2001). Since those initial discoveries there has been much work trying to understand, improve, and apply the performance of IPMCs and other EAPs.

1.2.2 Description of Ionic Polymers

Active materials are defined as materials that exhibit useful coupling between multiple physical domains (Leo, 2003). Electroactive polymers are a class of active materials. Polymers labeled as EAPs have a mechanical response to electrical stimulation and produce an electric potential in response to mechanical stimulation. EAPs are divided into two categories, electronic, driven by electric field, and ionic, driven by diffusion of ions. The research performed for this thesis uses ionic polymers. As stated, the electromechanical coupling in ionic polymers is ionic diffusion, specifically the motion of mobile cations. Ionic polymer material has both fixed anions and mobile cations. When the material is hydrated the cations will diffuse toward an electrode on the materials surface under an applied electric field. Inside the polymer structure, anions in interconnected clusters provide channels for the cations to flow toward the electrode. This motion of ions causes the structure to bend toward the anode (Bar-Cohen, 2001). Conversely, bending the ionic polymers will force ion diffusion and produce voltage, which can be measured or collected through the electrodes.

The specific type of ionic polymers used are ionic polymer-metal composites, which consist of a base polymer coated with a metal to act as surface electrodes. Typically the base polymer is one of the following, perfluorinated alkenes with short side-chains of ionic groups or styrene/divinylbenzene-based with substituted ionic groups. Perfluorinated alkenes have large polymer backbones and the side chains provide the ionic groups which interact with a solvent to produce the "active" characteristic. Styrene polymers take ionic groups from the phenyl rings to produce the "active" mechanism (Shahinpoor and Kim, 2001). The base for the IMPCs used in this research is Nafion®, which is a perfluorosulfonic acid polymer.

Electrodes must be added to the polymers before they can be used as active materials. The current manufacturing procedure involves an initial compositing process and then an electroding process. During the first step, polymers are placed in a metal salt bath so that metal-containing cations can diffuse into the material. With initial metal ions in place, a

reducing agent is added to grow the metal into a plating that coats the surface. The metal particles are concentrated near the surfaces of the polymer. The finished IPMC is effectively three layers, a large polymer layer sandwiched between two polymer-metal composite layers (Shahinpoor and Kim, 2003).

The electromechanical coupling of EAPs is characterized by high strain, low stress, fast reaction speed, and low drive voltage. Because the base material is a polymer, ionic polymer actuation can range to strains of >10%. The extremely large motion relative to size makes the polymers attractive as acutators. However, there is a tradeoff with stress generation. Ionic polymers can only generate a few megapascals of blocked stress. Depending on the source this value ranges from <1 (Leo, 2003) to 3 MPa (Bar-Cohen, 2001). Stress generation is one of very few limitations of the actuation mechanism. Reactions speeds of EAPs are as low as a few microseconds, but can range to minutes. Also, EAPs only require a few volts for actuation, usually less than 10 V (Bar-Cohen, 2001). Because of large strains, quick reactions, and low voltages researchers are working to find niche applications for EAPs.

1.2.3 Applications as Actuators and Sensors

Current research is working to find applications for ionic polymers in both the sensing and actuation mode. It is believed that applications can be found that take advantage of the inherent properties of the polymers and not be limited by the low force production. Some of these example applications are highlighted in the following section (Shahinpoor and Kim, 2005).

The high strains of IPMCs make them attractive as mechanical actuators for applications requiring large motion but little force. Two IPMCs can be made into grips by having them actuate in opposite directions. Also, three-dimensional actuators have been constructed by joining three individual polymers aligned in different actuation directions. Polymers have also been used to mimic the swimming or flapping motion of fins and wings. The use of polymers as fins is intriguing since most fins are used for balance or stability, not propulsion. Therefore, it is the position of the fin that matters, not the force generated, making the high strain polymers well suited to perform the function. Other industrial applications range from pumps and valves to electromechanical relay switches to musical instruments.

Many biomedical applications are being explored for ionic polymers. This area could benefit from the ability to manufacture tiny polymer actuators. Also, since the ionic polymers require a solvent, the hydrated human body provides a natural environment. Work is being performed to use ionic polymers as assist muscles for organs such as the heart and eyes. Polymers would be actuated to contract, assisting the heart to pump, or correcting the shape of the eye to improve vision. Another use is as miniature surgical tools that can be inserted inside the body. Possibly the biggest biomedical use would be as artificial smooth muscles, one of the original ideas for EAPs. These muscles could be placed in exoskeletal suits for soldiers or prosthetic devices for disabled persons.

Ionic polymers can be incorporated into micro electromechanical systems as sensors and actuators. The ability to easily manufacture large quantities of ionic polymers and make them almost as small as desired shows promise for MEMS applications. Sensors and actuators tend to be the most unreliable component of sensory-actuator-electronics, so IPMCs could potentially lower the cost and improve the reliability. MEMS technology is extremely diverse, so pairing IPMCs with MEMS could lead to applications in many different areas and products.

1.3 Energy Harvesting Technologies

1.3.1 Piezoelectrics

Description of Piezoelectric Materials

Like ionic polymers, piezoelectric materials exhibit a coupling between their mechanical and electrical domains. And while ionic polymers belong to a larger class of materials, EAPs, piezoelectrics are a type of ferroelectric material. The structure of ferroelectric materials contains electric dipoles, a positive and negative charge separated by a fixed distance. When an electric field is applied, the grains of the structure expand along the dipole direction and contract in the lateral direction. Originally the dipole orientation is randomly distributed throughout the material, but by poling the material the dipoles can be aligned. Dipoles are aligned by heating the material above the Curie temperature and applying an electric field. The cation moves in the direction of the field and the anion opposes it. The material is then cooled, producing the permanent alignment of the material. The poling process gives the ferroelectric material its electromechanical coupling by allowing all of the grains to move in

one direction when actuated (Gonzalez et al., 1998).

The electromechanical coupling works in two directions in piezoelectrics just as in ionic polymers. The sensor path, applying a mechanical stress and producing an electric charge, is called the direct piezoelectric effect. The motor path, applying an electric field to produce a mechanical displacement, is called the converse piezoelectric effect. Piezoelectrics are typically actuated in one of two ways, along the poling direction or perpendicular to the poling direction. When actuated along the poling direction, the configuration is referred to as a stack. The material will expand in the poling direction and contract in the other directions. Multiple layers of material can used to amplify this effect. Actuation perpendicular to the poling direction can be used to produce a bending motion. A piezoelectric bender or bimorph uses two pieces of material bonded together in a configuration where an applied electric field will cause expansion of one piece and contraction of another. Because the pieces are bonded, the material bends (Leo, 2003).

Piezoelectrics have the opposite electromechanical coupling characteristics of ionic polymers. Piezoelectrics produce low strain, but large stress. Typical strains for piezoelectrics are between 0.1 and 0.3%, while generated stress ranges between 30 and 40 MPa. Another difference between the ionic polymers and the piezos is the drive voltage. Ionic polymers can be activated with low voltages, but piezoelectrics require anywhere from 50 to 800 V to cause actuation. The only property that is similar is the reaction speed, a few microseconds for both materials (Bar-Cohen, 2001).

Differences in the characteristics of the piezoelectrics are attributable to the base material. Most of the piezoelectrics used for engineering purposes are ceramic. It is expected that ceramics would produce less motion than polymers since they are more rigid. However, because they are a more rigid structure they can produce larger forces. Typically, piezoceramic sheets have a elastic modulus of 50 GPa in the poling direction and 62 GPa in perpendicular direction (Piezo Systems, 2005). That is approximately two to three orders of magnitude larger than ionic polymers.

Piezoelectric Power Generation

Power generation with piezoelectrics has been pursued via two different methods. The first method excited the material by simulating vibrations produced by an automobile. Vibrations are the most common source of energy for exciting the material to exploit the

energy harvesting potential. The material can be attached to any machine or vehicle that has significant vibrations. The second method compresses the material. Compression was achieved in two ways, impacting the material and using a rapid deceleration.

Piezoelectric power generation from ambient vibrations has shown potential for producing usable power. Various vibration sources have been explored including vehicles and humans. Promising results were shown by simulating the magnitude of vibrations produced by a automobile compressor. The piezoelectric material is excited with a chirp signal to obtain data at different frequencies. Maximum power produced is approximately 2 mW, occurring at the natural frequency of the piezo. Average power is in the range of 0.2 mW. Also demonstrated is the ability to charge a battery with the harvested power. At resonance the piezoelectric material is able to charge a 40 mAh battery in one hour. Using a random signal, similar to the car compressor, the charging time climbed to 1.5 hours (Sodano, 2003).

The other method for straining the material is compression, using impacts to create a pulse generator. The compression force is input in two ways, dropping a mass on the material for approximately 10 kN of force and imparting a deceleration for approximately 20 kN. This method was able to generate maximum power pulses of 320 kW, but with lengths of 0.5 μs. This is significantly less than the vibration method since the average power can be sustained for as long as the vibrations are sustained. However, this study did conclude that power is scalable with the volume of the piezoelectric device (Keawboonchuay and Engel, 2004).

1.3.2 Electromagnetic Devices

Description of Electromagnetic Devices

Electromagnetic devices use the motion of a magnet relative to a wire coil to generate an electric voltage. A permanent magnet is placed inside a wound coil. As the magnet is moved through the coil it cause a changing magnetic flux. This flux is responsible for generating the voltage which collects on the coil terminals. This voltage can then be supplied to an electrical load (Duffy and Carroll, 2004). Because an electromagnetic device needs a magnet to be sliding through the coil to produce voltage, energy harvesting through vibrations is an ideal application.

Electromagnetic Power Generation

Two different studies are discussed to exemplify electromagnetic power generation. Both studies focus on producing power from the motion of human beings. Also, both studies produced several milliwatts of power. The first study tested the electromagnetic device at resonance frequency and with optimal loading. This device was able to produce a maximum of 2.5 mW (Poulin et al., 2004). A second study actually produced electromagnetic devices that fit inside the heel of a shoe. One a sliding magnet-coil design, the other, opposing magnets with one fixed and one free to move inside the coil. The first device was able to produce 8.5 mW and the second 0.23 mW (Duffy and Carroll, 2004). While both designs were able to produce milliwatts of power, this production is dependent on the dimensions of the device. If the length of the coil is increased, which increases the turns, the device is able to produce more power.

1.4 Thesis Overview

1.4.1 Contribution

The purpose of this thesis is the development and analysis of applications for ionic polymers as energy harvesting devices. The worked focused on addressing the specific power harvesting need for the condition-based health monitoring and wireless communications discussed in the Motivation section. The specific application for mounting the energy harvesting device on ship propulsors incorporated strict environmental guidelines including the the frequency of the vibrations, loading magnitudes, and dimensions. Using the design requirements, an ionic polymer device was developed to function in the described environment as an energy harvester. The device uses the dynamics of the environment and the properties of the ionic polymers to convert mechanical energy to electrical energy. Design curves have been generated to describe the mass, stiffness, size, and stresses for various options of the design. The selected design was then characterized to determine the amount of electrical energy that could be harvested by mechanically exciting the device. Transfer functions were collected to quantify the open-circuit voltage and closed-circuit current. Data was collected for frequencies up to 500 Hz. The impedance of the device was also measured for the same bandwidth. The expected power that the ionic polymer device could produce was calculated using the voltage and current. The power calculation included adjusting

for the increased resistance from matching the impedance of the polymer device to the required rectifier circuit. Therefore, the power calculated is the actual power expected after the raw AC signal has been converted to a DC supply. Along with the energy generation device, ionic polymers were also considered as the energy storage vessel for the harvesting application. The capacitive characteristics of the design were investigated for the purpose of using the polymers in place of a standard capacitor bank. The ionic polymer device was tested to determine the charge and discharge characteristics, which were then compared to commercial capacitors. The research has explored the energy harvesting application of ionic polymers and concluded that while ionic polymers do not produce large amounts of electrical energy, they do show potential for storing significant amounts of electrical energy. Using the polymers as specialized capacitors is a real possibility.

1.4.2 Approach

A detailed design process is presented in Chapter 2. The design requirements are discussed along with the process for developing the design curves and selecting the final design. Chapter 3 describes the testing procedures and presents the experimental results of the ionic polymer energy harvesting device characterization. Also included in Chapter 3 are the power calculations and an examination of the transfer functions obtained during testing. The energy storage testing and results are presented in Chapter 4 along with a comparison of the storage ability of ionic polymers and commercial capacitors. Chapter 5 presents the conclusions of the research and provides recommendations for future work.

Chapter 2

Design of Power Harvesting Device

The concept of the Phase I energy harvesting device is an arrangement of ionic polymer membranes that will convert mechanical energy into electrical energy. Two posts, made of individual polymer membranes, will support a head mass that induces strain when the system is exited by the revolutions of the propeller. Figure 2.1 illustrates the original concept. When mounted on the propeller, the axial direction in the figure is the radial direction of the propeller. Oscillations in the lateral direction will produce the recurring strain in the material. Specific requirements were given for size, loading, and operating frequency range. These design parameters are listed in Table 2.1. The ionic polymer energy harvester will be packaged in a cylindrical container that has already been designed. Only 75% of the cyclinder volume is available for the harvester. The remaining space is reserved for electronics necessary for collecting the harvested energy. Loading and frequency range estimates are based on assumptions of the specific application of the device.

Design of the device concentrated on four areas, maximizing the strain of the polymers, tuning the device to the selected frequency, packaging the device within the specified container, and assuring the survival of the device under the assumed loads. However, each area of the design affects the other areas. The mass needed to strain the polymers affects the stiffness and strains. Stiffness affects the stroke, which interferes with the packaging. Packaging dictates the maximum size of the device which constrains the amount of mass. To combat this circular effect, design curves were generated for each area of the design to provide options. Comparing the design curves allowed a solution to be selected that meets all of the requirements and constraints of the environment.

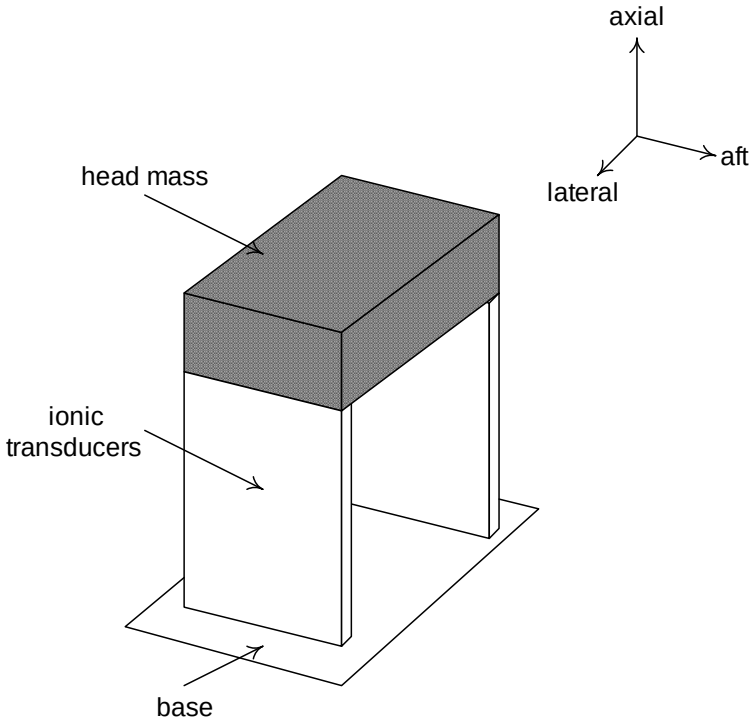

Figure 2.1: Original concept design for the ionic polymer energy harvester.

Table 2.1: Design parameters for the Phase I ionic polymer energy harvester.

Package Size: Outside Dimensions	6.35 cm dia. $\times$ 7.62 cm (241 cm^3)
Package Size: Inside Dimensions	5.72 cm dia. $\times$ 6.86 cm (176 cm^3)
Available space for energy harvester	132 cm^3
Axial (Radial) Acceleration	0 - 100 Gs
Lateral Acceleration	$\pm$ 1 G
Operating Frequency Range	0.2 - 4.2 Hz

2.1 Maximizing Strain of the Polymers

Ionic polymers convert mechanical energy to electrical energy with a nearly linear relationship (Newbury and Leo, 2002, 2003a,b). To make the energy harvester efficient the polymers should experience the largest possible strains. Ionic polymers can sustain strains greater than 10% without failure, but for this design the limit is set at 10% (Shahinpoor and Kim, 2001). This provides adequate strain on the material and also provides a level of safety in the design. The harvester device experiences loading in both the axial and lateral directions. Axial loads are assumed to be a constant 100 Gs during operation and lateral loads are assumed to be ±1 G. Since the axial loading is much greater, it determines the required mass.

The size of the polymer posts is varied to provide design options requiring mass to be calculated for each option. Number of layers and width of the polymer samples are varied in the mass calculations. For the calculation each polymer post carries half of the load, so the forces in either direction can be calculated with the following expression,

$$F_{dir} = \frac{1}{2} m_h \alpha_{dir}. \tag{2.1}$$

To simplify the calculation the post is assumed to be solid. To justify this assumption the polymer posts will be encapsulated and embedded into the head mass and base of the device. The encapsulation will stop the individual samples comprising the post from separating and having each end of the post embedded will minimize the layers slipping past one another. Combining the following two equations (Beer and E. R. Johnston, 1992),

$$\epsilon = \frac{\delta}{l}, \tag{2.2}$$

$$\delta = \frac{F_a l}{AE}, \tag{2.3}$$

with equation 2.1 provides an expression for the necessary mass,

$$m_h = \frac{2\epsilon_a wtE}{\alpha_a}. \tag{2.4}$$

For these calculations the modulus, E, is 249 MPa, which will be verified later. The results of the mass calculation are shown in Figure 2.2. Smaller widths and fewer layers reduce the amount of mass required to produce the desired strain.

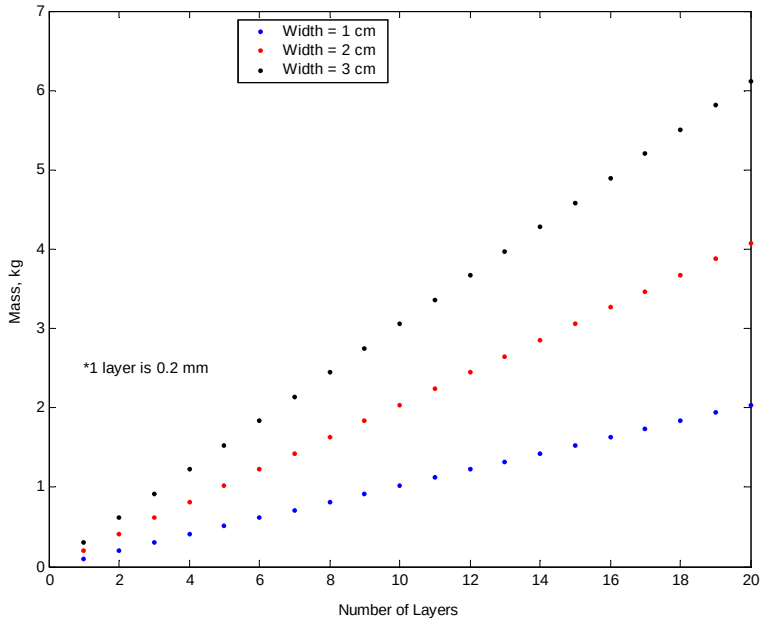

Figure 2.2: Curves for predicting amount of mass needed for 10% axial strain of polymer material.

2.2 Frequency Tuning

Operating frequencies for the device are between 0.2 and 4.2 Hz. Tuning the harvesting device to the proper frequency creates limits in the design since the frequency is so low. To tune the device to these low frequencies requires the polymer posts to have a low stiffness. However, a relatively flexible post will have large deflections that could interfere with the device's container. To increase stiffness the harvester device is tuned to a frequency of 7 Hz. Designing to this higher frequency also avoids resonant effects which would amplify the deflections.

Again, a curve is generated to predict the stiffness required when the amount of polymer material is varied. A stiffness that will tune the device to 7 Hz is calculated for each mass shown in Figure 2.2 using the following equation (Inman, 2001),

$$k_d = m_h \omega_n^2. \tag{2.5}$$

The calculated stiffness follows the same trends as the mass. When the amount of material is increased the stiffness is increased. Again, using less material is shown to be beneficial. Figure 2.3 shows the stiffness curves.

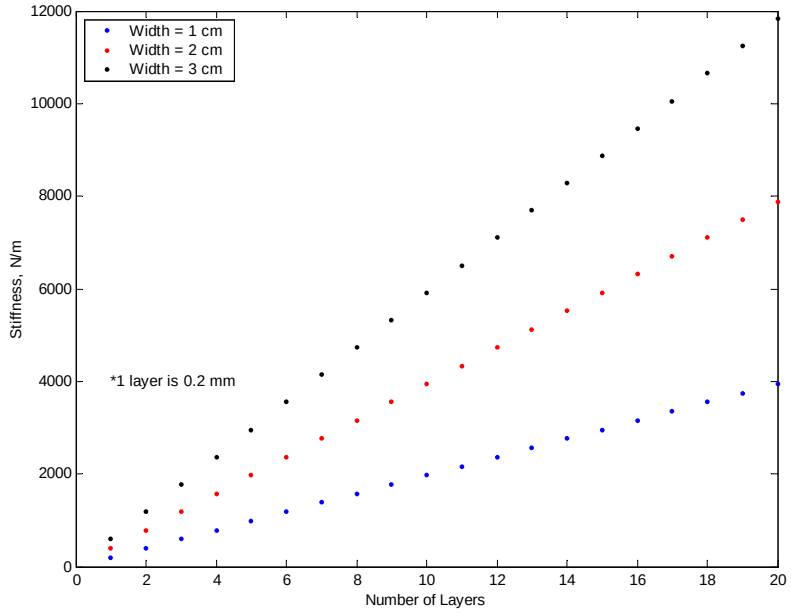

Figure 2.3: Curves predicting the required stiffness to tune the device to 7 Hz.

2.3 Packaging the Energy Harvester Device

The harvester device will be packaged in a container that has already been designed. The container has an inside length of 6.86 cm and an inside diameter of 5.72 cm. There is approximately 176 cm^3 of available space inside the container; however, the harvester device must share the space with the necessary electronics. Seventy-five percent or 132 cm^3 has been designated for the ionic polymer harvesting device. So realistically the harvester device, which includes the base, polymer posts, and head mass, can only have a total length of 5 cm.

The length of the polymers is independent of width so the only design option considered for this calculation is the number of layers. Stiffness for a two-beam support is calculated with the following equation (Blevins, 2001),

$$k_d = \frac{12E(I_1 + I_2)}{l^3} \tag{2.6}$$

where I, with both posts having the same geometry, is (Beer and E. R. Johnston, 1992),

$$I = I_1 = I_2 = \frac{1}{12}wt^3. \tag{2.7}$$

Rearranging these relationships, it was possible to calculate the free length of the polymers,

l, from equation 2.6,

$$l = l_f = \sqrt[3]{\frac{2Ewt^3}{k_d}}. \tag{2.8}$$

The free length of the polymers needed for the various design options is shown in Figure 2.4. The total length of the polymer will be larger since both ends will be embedded.

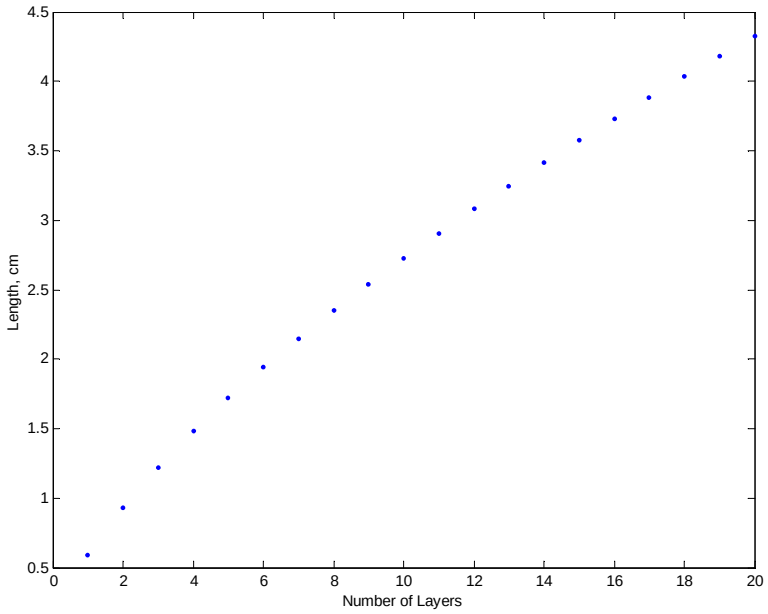

Figure 2.4: Free length of the polymers required to produce the target stiffness for the design options.

2.4 Stress Calculations

Stress calculations are critical to the design to insure the survival of the device under operating conditions. The ionic polymers are made from Nafion®N-117 that has been impregnated with noble metals. Since Nafion®is a commercial polymer, the material specifications are well known (DuPont^{TM}, 2004). Specification sheets list three different values for allowable stresses based on the level of hydration of the material, 50% relative humidity, water soaked at 23°C, and water soaked at 100°C. To determine which allowable stresses are appropriate, the material was placed in design configuration, both ends clamped to simulate a post, and tested to determine the elastic modulus. The modulus of the material is also dependent on the level of hydration, so it will indicate which stress level is acceptable.

Elastic modulus is not measured directly, but derived from the stiffness of the material. A random signal is used to impart motion to the polymers while the opposite end of the sample is constrained with a load cell. A potentiometer measures the motion and the load cell measures the corresponding force generated by the polymers. This provides the stiffness transfer function,

$$k(\omega) = \frac{f(\omega)}{u(\omega)}. \tag{2.9}$$

The modulus is derived from the stiffness using the following equation (Newbury and Leo, 2003a),

$$E(\omega) = \frac{4k(\omega)l^3}{wt^3}. \tag{2.10}$$

Five different samples were tested and the results are shown in Figure 2.5. The same batch of ionic material tested for modulus will be used to fabricate a model of the selected design to insure consistent results.

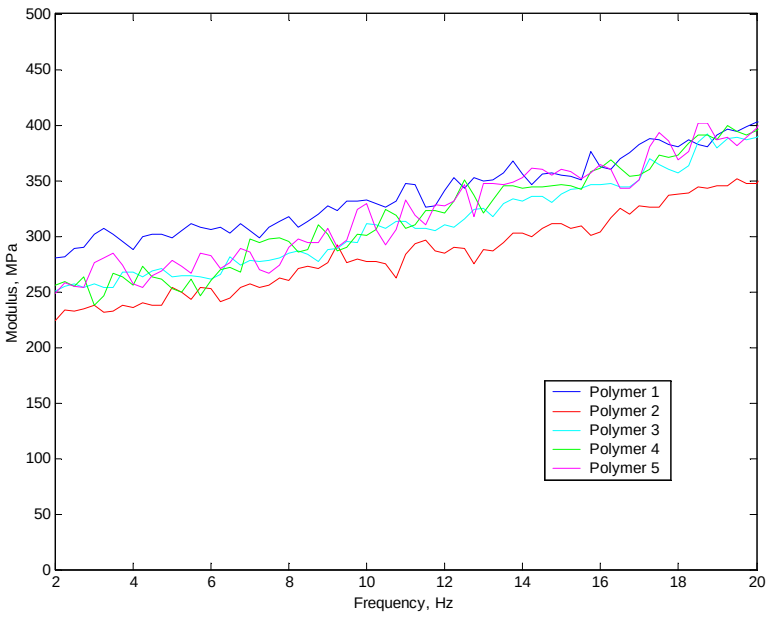

Figure 2.5: Elastic modulus of the ionic polymers.

Polymer materials have a frequency dependent modulus because of the viscoelastic behavior of the material. These ionic polymers have an elastic modulus of approximately 260 MPa at the target frequency of 7 Hz. Nafion®N-117 specifications list the modulus to be approximately 249 MPa at 50% relative humidity, which matches well with the test results. Results show that at extremely low frequencies, 0-2 Hz, the modulus is 249 MPa.

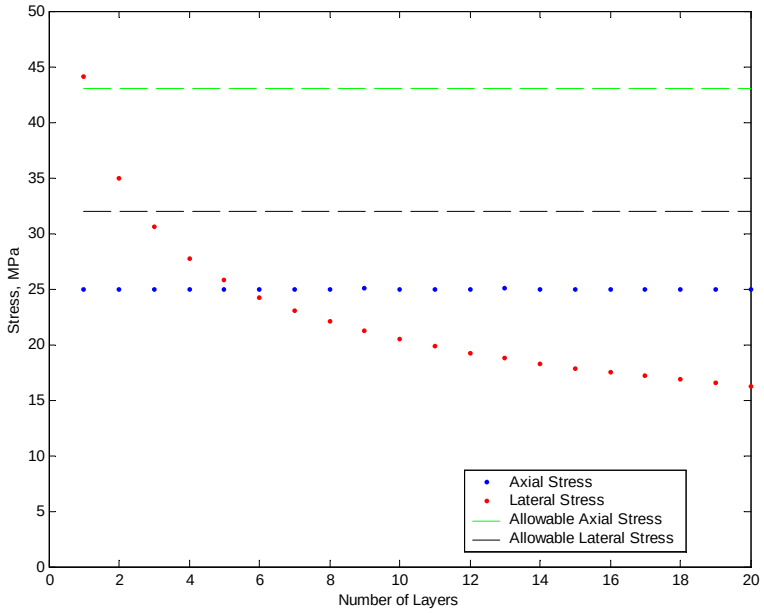

Figure 2.6: Calculated stress curves and allowable stresses for the polymer posts.

Based on the material specification sheets, and validated by the modulus test, the polymers have an allowable tensile (axial) stress of 43 MPa and an allowable transverse (lateral) stress of 32 MPa (DuPont^{TM}, 2004).

Using the mass curve, stress curves are calculated to predict the stresses seen in the polymers for each design case. The stress in the axial and lateral directions were calculated with these relationships (Beer and E. R. Johnston, 1992),

$$\sigma_a = \frac{F_a}{wt}, \tag{2.11}$$

$$\sigma_l = \frac{\frac{1}{2}F_l lt}{I}. \tag{2.12}$$

The stress curves are shown in Figure 2.6 with the known allowable stresses shown as well. While there are three mass curves, one for each width, there is only one stress curve for each deflection direction. This occurs since the ratio of mass and geometry is constant between the curves. Calculated axial stress in the polymers is constant since the mass is designed to produce 10% strain in that direction. Calculated lateral stress shows an exponential decrease as the number of layers in the polymer posts is increased. As layers are added to the post, the lateral strain of the post is decreased as are the stresses.

2.5 Selected Design for the Energy Harvester Device

Using the design curves discussed in the previous sections it is possible to select a design for the energy harvester that will meet all of the design criteria. A smaller width benefited the design, requiring less mass, so only the 1 cm width option is considered. Using more than 10 layers will require almost 1 kg of mass, which is too large to package, so these options are also discarded. Finally, the stress curves show that at least three polymer samples must be used in each post. The available range for the device is between 3 and 10 samples per post. A design from the high end of this range is preferred since more ionic material will convert more mechanical energy to electrical energy.

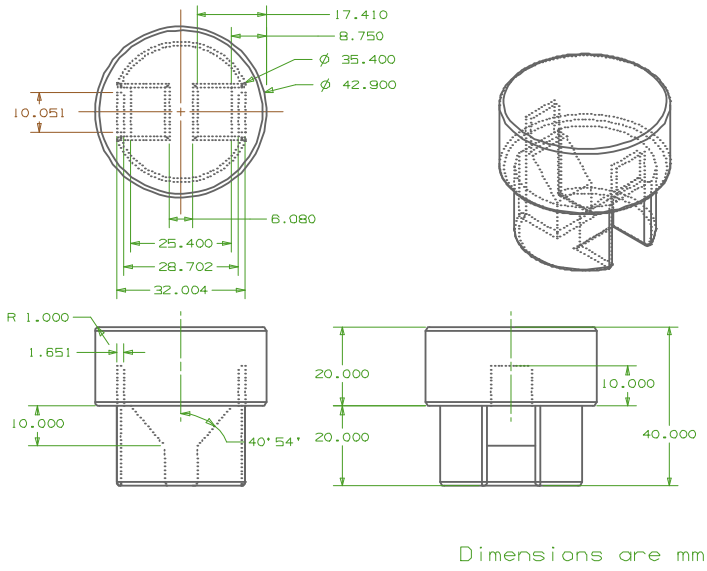

Figure 2.7: Detailed design of the head mass.

From the usable range the 8-layer polymer post is the best option. After experimenting with the options and the design of the head mass, the 8 layer post allows for the most ionic material to be in the design while the stroke of the device does not interfere with the container. A mass of 0.816 kg and a stiffness of 1577 N/m correspond to the 8 layer post. To conserve space the head mass will be made from a dense material, specifically Tungsten which has a density of 19250 kg/m^3. The polymer posts have a 2.35 cm free length, a 1 cm width, and a total thickness of 0.16 cm. Length was added to the individual polymer samples so that they could be embedded and secured properly in the design. Each individual polymer sample will have the following dimensions, 3.85 cm, 1 cm, 0.02 cm. Figures 2.7,

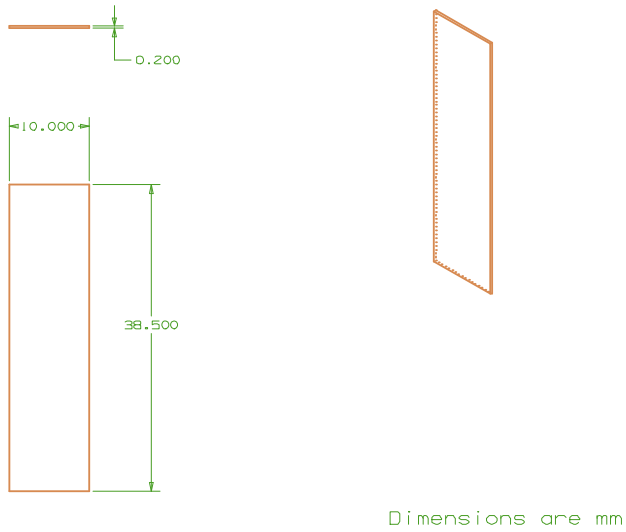

Figure 2.8: Detailed design of the individual polymer samples.

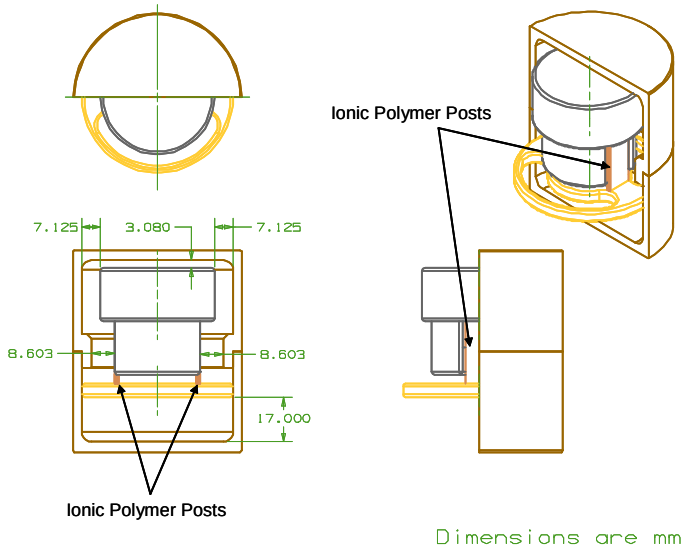

Figure 2.9: Fully packaged energy harvester. One half of the packaging container has been cut away to show how the device fits.

2.8, and 2.9 provide detailed dimensions of the design.

Under the assumed loading the dynamic forces placed on the device will be 800 N in the axial direction and ±8 N in the lateral direction. These forces will produce stresses of 25 MPa and 22 MPa in the axial and lateral directions, respectively. Assuming a modulus of 249 MPa, the strain in the lateral direction is ± 8.8%. This represents a lateral stroke of ±0.507 cm.

Clearance for the device at maximum stroke is 0.2 cm in the lateral direction. A 10% strain of the free length of the polymer in the axial direction produces a deflection of 0.235 cm. The harvester device design has a clearance of 0.073 cm after the maximum axial deflection.

2.6 Failure of the Energy Harvester under Loading

The harvester device will fail in two ways under the loading conditions. Combined axial stress is too great for the ionic polymers and the static weight of the head mass will cause the posts to buckle. The head mass needs to be supported by something other than the ionic polymers. A Phase II design will need to include some other support for the head mass. Possible options would be a post other than the polymers with the proper stiffness or a track that allows the mass to slide but also provides support. Other possible options would be to decrease the axial strain reducing the axial stress or to increase the target frequency. Less direct axial stress will lower the combined stress. A higher target frequency will increase the stiffness, which will also reduce the stress.

2.6.1 Combined Axial Stress

The maximum combined axial stress occurs in the polymers at the peak of the stroke. At this point the fibers carry both the maximum axial load and maximum lateral load. The combined stress, shown in Figure 2.10, indicates that the design will fail if less than 16 polymer samples are used per post. However, using that many polymers for a posts will require the head mass to be too large to package.

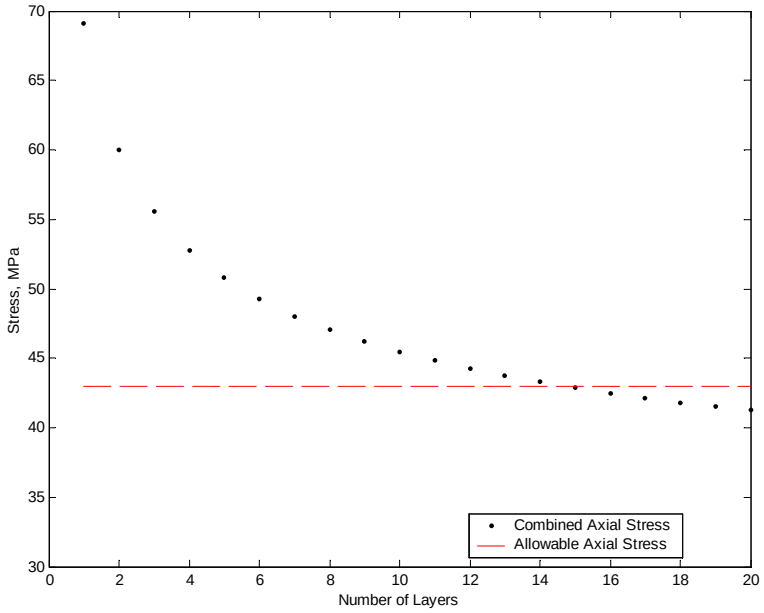

Figure 2.10: Combined axial stress in the ionic polymer samples at peak stroke.

2.6.2 Buckling

The design is analyzed for buckling under the static weight of the head mass. For the analysis each polymer post supports half the weight. The posts are first analyzed to determine the appropriate buckling region: compressive, Euler-Johnson, or Euler Buckling. Both area moments of inertia are calculated (Beer and E. R. Johnston, 1992),

$$I_x = \frac{1}{12} w t^3, \tag{2.13}$$

$$I_y = \frac{1}{12} w^3 t. \tag{2.14}$$

Buckling is assessed using the following procedure (Mischke and Shigley, 2001). The smallest moment of inertia is used to calculate the radius of gyration,

$$\kappa = \sqrt{\frac{I_x}{wt}}. \tag{2.15}$$

The slenderness ratio,

$$S = \frac{l_f}{\kappa} \tag{2.16}$$

is then compare with the tangent slenderness ratio,

$$(l/\kappa)_1 = \sqrt{\frac{2\pi^2 CE}{S_y}} \tag{2.17}$$

to determine the appropriate region. In equation 2.17, C is the end-condition constant, which in this case is fixed-free. The conservative value for C under these conditions is $\frac{1}{4}$. The Euler region is the appropriate region of buckling to consider based on the geometry of the polymer posts. Critical loading in this region is calculated with this formula,

$$P_{cr} = \frac{C\pi^2 Ewt}{(l/\kappa)_1}. \tag{2.18}$$

The amount of critical mass is calculated by dividing the critical loading by gravity. From the Euler buckling theory each post can support 0.387 kg of mass.

However, actual testing does not support these numbers. The proposed energy harvester design was tested statically to determine the actual amount of weight it can support. The stiffness of the proposed design, two posts in parallel sharing the load, is greater than the stiffness sum of two individual posts as illustrated by equation 2.6. It should therefore be able to support more weight per post than the theory suggests. In reality, the design buckles under less weight than calculated.

A Phase I model was placed in a test fixture and loaded to determine the actual weight it could support. For the buckling test the 8-layer polymer posts are encapsulated to prevent the layers from separating. Plastic wrap is wound around the polymers and then sealed by melting the layers of plastic together. When the posts are straight the device can support 0.23 kg, much less than the predicted weight. If the posts have any deflection, so the loading is eccentric, the allowable weight is decreased to 0.154 kg. Both values are significantly lower than the design weight of 0.816 kg. For Phase II additional support is needed.

2.7 Chapter Summary

In this chapter the design for an ionic polymer energy harvester has been presented. Design of the device concentrated on four areas, maximizing the strain of the polymers, tuning the device to the selected frequency, packaging the device within the specified container, and assuring the survival of the device under the assumed loads. Design curves were generated for each area to aid the choice of a suitable design. The design was based on finding a head mass and ionic polymer combination that would fit within the design constraints and also provide adequate strain on the materials. Using the design curves, a 16 layer ionic polymer design was chosen. The selected design was evaluated to quantify the axial and

lateral deflections as well as the axial and lateral strains. The clearance of the device inside the canister under loading was also calculated. The design can sustain the axial and lateral stresses independently, but fails under the combined stress. Buckling of the design is also an issue. Additional supports would need to be designed if the device was taken to a Phase II level. The next chapter presents the results of testing the design for power generation.

Chapter 3

Characterization of Power Generation

The feasibility of the proposed design is tested by building an engineering model, denoted EM1. The polymer samples are the same size as those proposed in the EM1 design, 3.85 cm $\times$ 1 cm $\times$ 0.02 cm. Two posts, constructed of eight individual polymer samples for a total thickness of 0.16 cm, are wrapped with plastic wrap to simulate the encapsulation. The polymer posts are clamped in a fixture that provides the same clamped-free boundary conditions. The polymers have a free length of 2.35 cm when placed in the fixture. Pictures of the test setup are shown in Figures 3.1 and 3.2.

Testing is performed on the ionic polymers in both sensing and actuation modes. Figure 3.3 provides diagrams of the experimental test setups. During voltage and current testing the material is placed in a sensing configuration, meaning no voltage is applied to the materials, only motion. A Tektronix 2630 Fourier Analyzer is used to supply the excitation signal and collect the data. A shaker excites the polymers and the signal is conditioned with circuits to a form compatible with the Tektronix. A Polytec OFV laser vibrometer measures the displacement of the polymers which is also collected by the Tektronix analyzer.

To obtain impedance data the polymers are placed in actuation mode. The shaker is removed from the fixture allowing the polymers to move freely when activated. A voltage is sent directly to the polymers from the Tektronix. This voltage as well as the current present in the polymer is measured. The Tektronix constructs a transfer function for the impedance based on the measured current caused by the voltage signal.

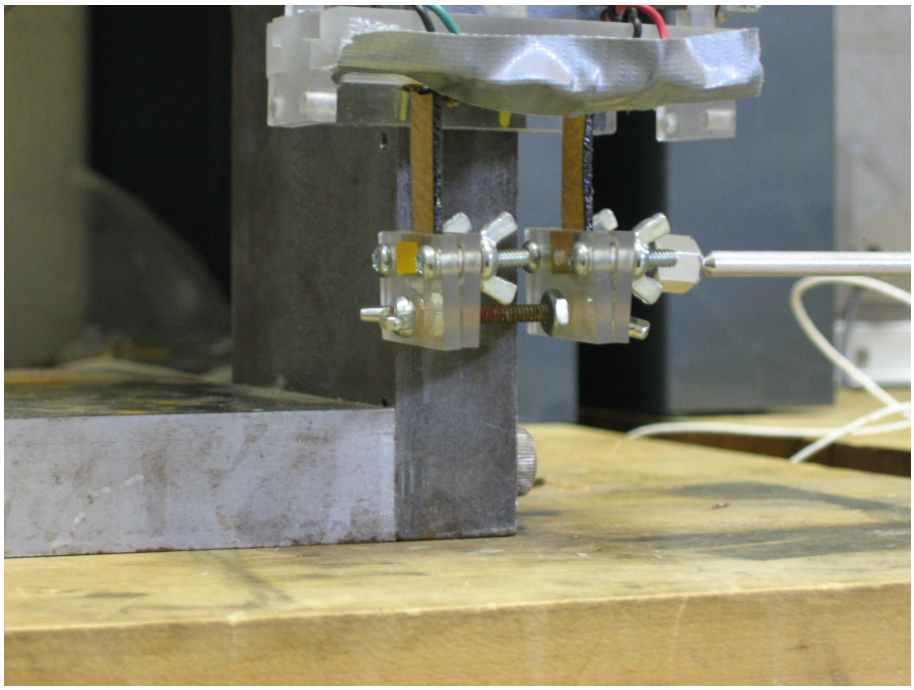

Figure 3.1: Ionic polymers in the test fixture.

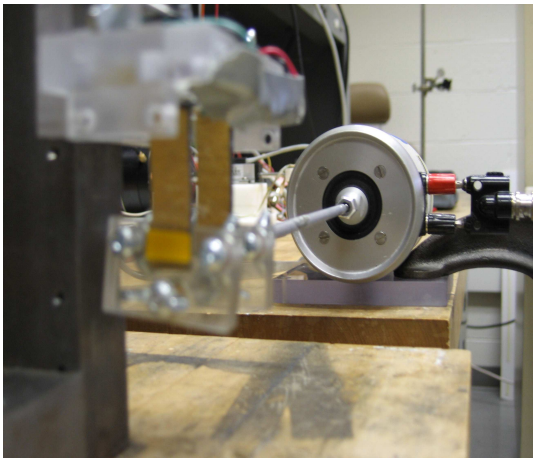

a)

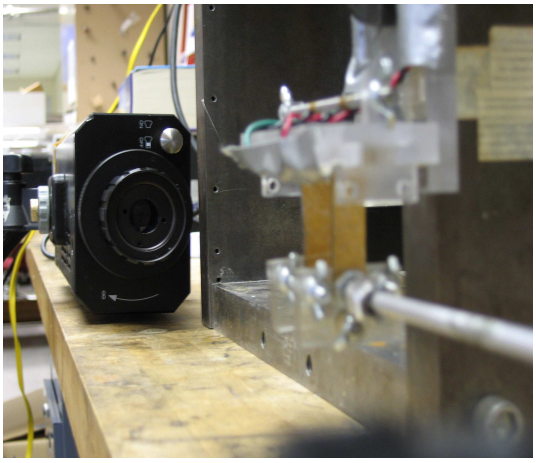

b)

Figure 3.2: Side views of the test setup: a) left view b) right view.

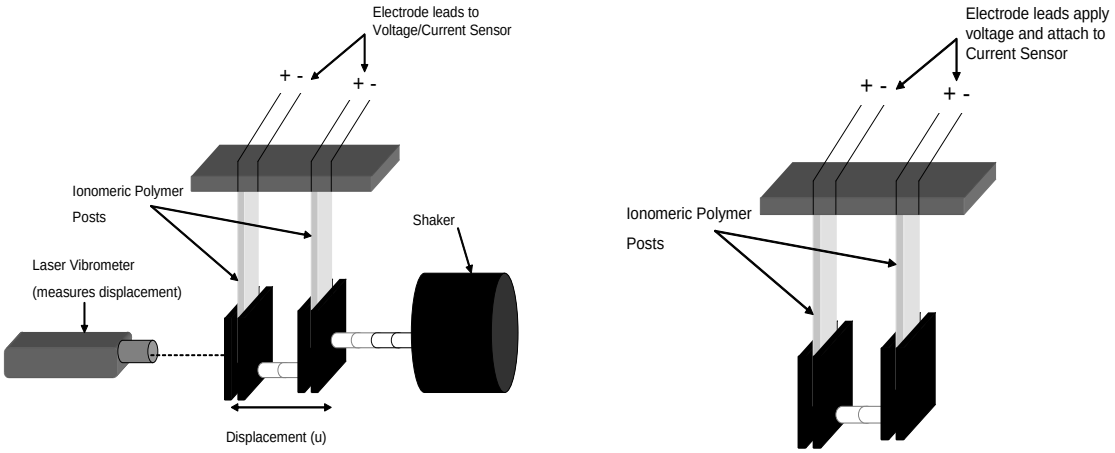

Figure 3.3: Diagrams of the experimental setups: a) sensing configuration b) actuation configuration.

3.1 Open-circuit Voltage

Open-circuit voltage produced by the polymers is measured. Placing the polymers in the open-circuit configuration ensures the largest voltage possible because there is an infinite resistance, which is equivalent to having zero electrical loading on the polymers during testing.

A transfer function of the voltage sensitivity is collected to determine how much voltage the ionic polymers will produce at certain frequencies. The voltage sensitivity, $V(\omega)$, is described in the following equation,

$$V(\omega) = \frac{v_o(\omega)}{u(\omega)} \tag{3.1}$$

where, $v_o(\omega)$ is frequency dependent voltage and $u(\omega)$ is the induced displacement. The polymers are layered in series so voltage will add. To collect the transfer function EM1 is excited with a 1.812 Vrms random signal. The voltage sensitivity transfer function is shown in Figure 3.4. Near the target frequency the ionic polymers produce approximately 3.8 mV/cm. Therefore, the voltage produced by the proposed design of EM1, with a calculated stroke of ± 0.507 cm, is ± 1.9 mV. One complete stroke of EM1 at the target frequency will produce approximately 3.8 mV. However, the transfer function shows that the polymers are frequency dependent in energy production. The voltage produced by EM1 will change if the frequency of the loading changes.

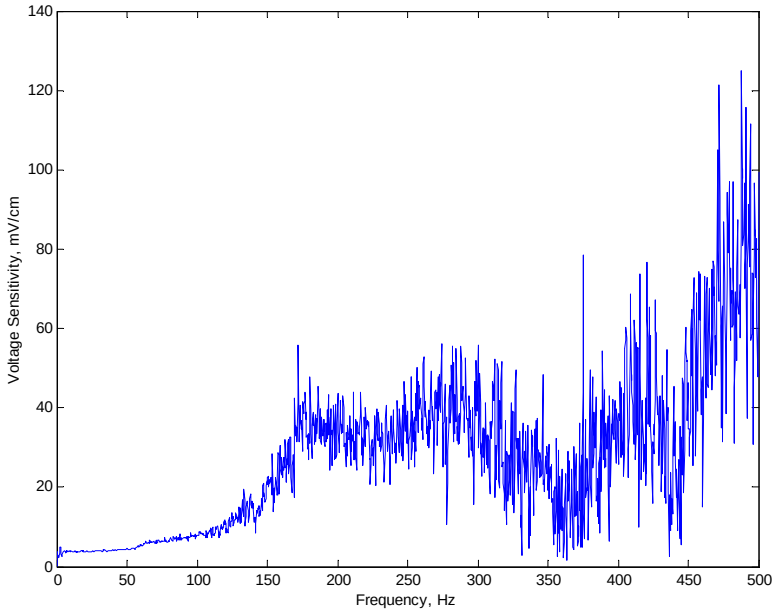

Figure 3.4: Open-circuit voltage sensitivity transfer function for the EM1 test model.

Open-circuit voltage is tested for each individual sample and then for multilayer stacks comprised of the samples. The stacks range from two to eight layers. Polymer samples are stacked so that they connect in series. The individual voltages are shown in Figure 3.5 for all sixteen polymers. While there is a little scatter, the voltage transfer functions all lie in the same range. Therefore, all of the samples are working properly meaning a damaged sample did not effect the voltage characterization. Figure 3.6 shows the results of the open-circuit voltage test for multilayer stacks. Voltage production does not increase linearly with increasing layers. Generally the production increases, but some of the data appears to be out of order, such as stacks 1-6 and 1-8. The reason for these irregularities is that the testing procedure has some inherent errors. First, the polymers must be taken out of the test fixture when a layer is added. It is impossible to reset the test fixture exactly the same every time. The larger factor is the connection between the polymers. Wrapping is applied to the outside to contain the entire stack, but there is nothing attaching the individual layers to one another. When excited the layers slide past each other. Depending on how tight the outside wrap is, the friction between layers could change and effect the strain, which effects the voltage production.

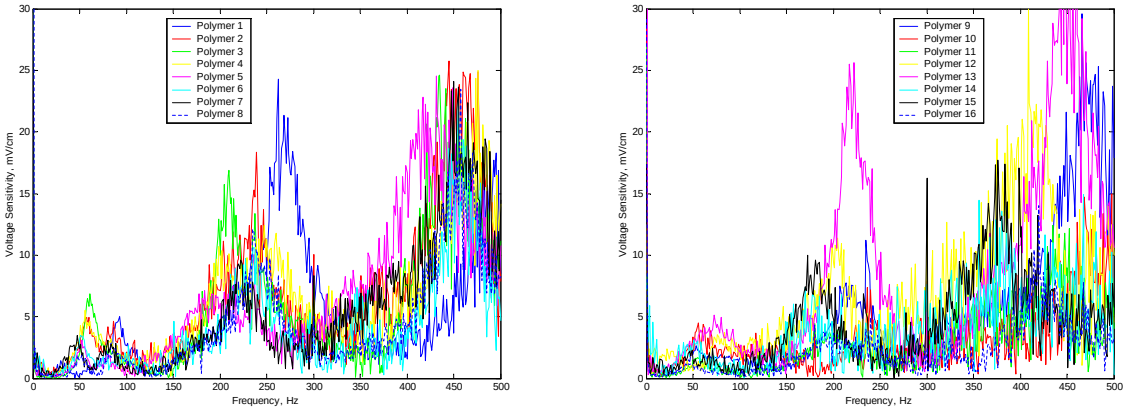

a) b)

Figure 3.5: Open-circuit voltage transfer functions for the individual polymer samples.

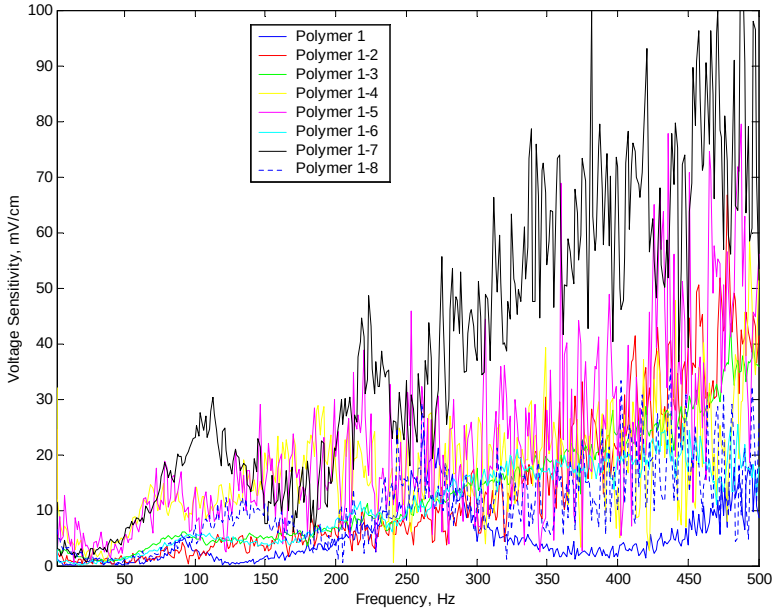

Figure 3.6: Open-circuit voltage transfer function for multilayer stacks. The plot shows the irregularities in voltage production due to changing connection conditions between the layers.

3.2 Closed-circuit Current

The current measured in the polymer samples is closed-circuit current. A short circuit has no resistance, allowing the maximum current to be measured. Again, this is done so that there is no electrical loading of the polymers during testing.

The current sensitivity transfer function is collected using the same method as the voltage transfer function. The current sensitivity, $I(\omega)$, is described in the following equation,

$$I(\omega) = \frac{i_c(\omega)}{u(\omega)} \tag{3.2}$$

where, $i_c(\omega)$ is frequency dependent current and $u(\omega)$ is the induced displacement. A 1.812 Vrms random signal excites EM1 and the resulting current is measured. A transfer function of the close-circuit current is shown in Figure 3.7. Near the target frequency EM1 produces approximately 4.5 μA/cm of current. For the predicted deflection this is $\pm$ 2.3 μA or 4.6 μA per complete stroke. However, this could vary since the current is also frequency dependent.

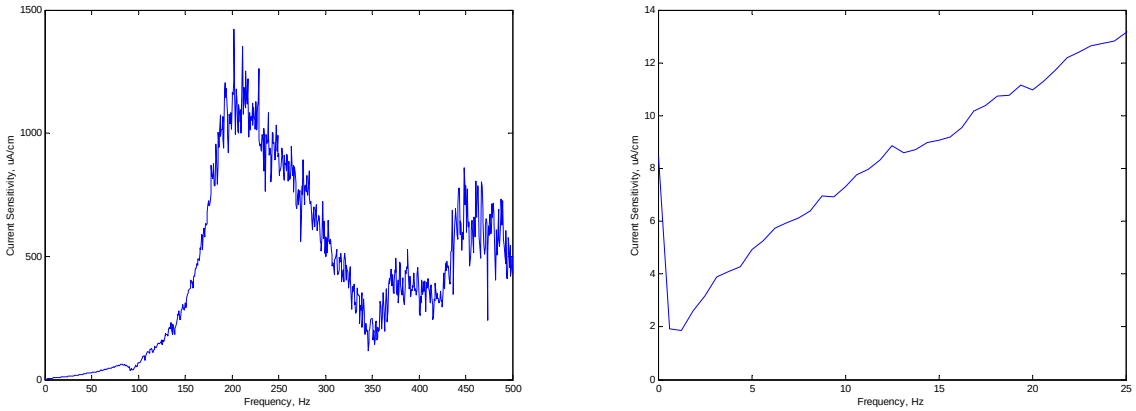

a) b)

Figure 3.7: Closed-circuit current sensitivity transfer function of EM1: a) full bandwidth b) low frequencies.

Individual samples are also tested for closed-circuit current production. The procedure is the same as for the voltage, each sample is tested individually and then stacks of up to eight layers are also tested. The individual results are presented in Figure 3.8. Since the polymers are layered in series the current should stay relatively constant, which Figure 3.9 supports. While there is some scatter, it is caused by the changing internal conditions of the stack.

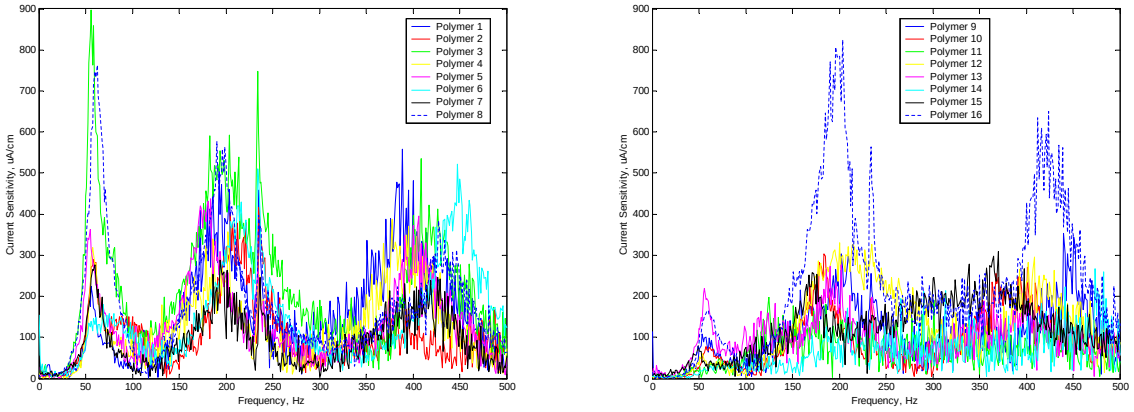

a) b)

Figure 3.8: Closed-circuit current transfer functions for the individual samples.

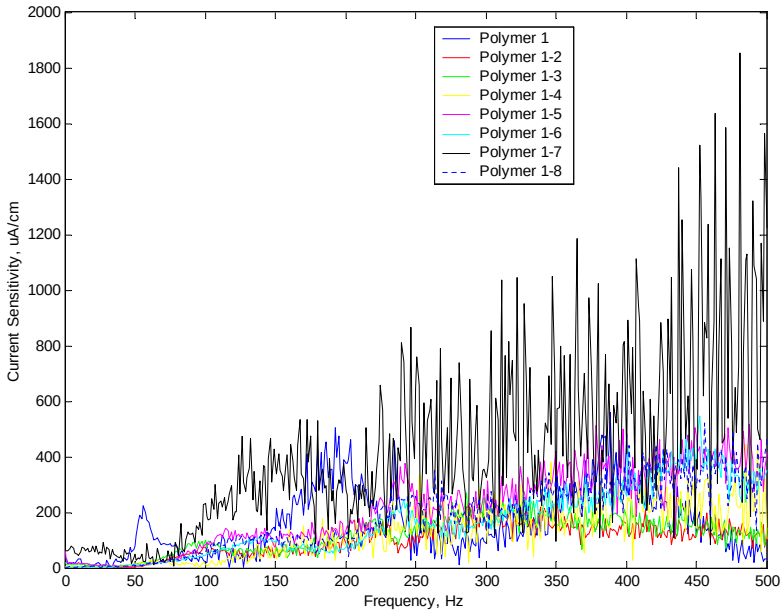

Figure 3.9: Closed-circuit current sensitivity for multilayer stacks.

3.3 Impedance

The impedance of the ionic polymer posts designed for EM1 is important for the power harvesting application. To maximize the power collected by the rectifier circuit, the impedance of the circuit must be matched to that of the transducer device. If the impedance of the source and the load are not matched part of the energy is reflected.

Impedance data is collected using the same signal that is used to collect the sensing data. A 1.812 Vrms signal is applied to EM1 and the resulting current is measure. The ratio of the two values is the impedance of the device,

$$Z(\omega) = \frac{v(\omega)}{i(\omega)}. \tag{3.3}$$

Figure 3.10 shows the impedance transfer function for EM1. Impedance of the ionic polymers is very high at low frequencies, typically on the order of hundreds of Ohms. Examining the impedance transfer function reveals that the impedance of EM1 is approximately 800 Ω at the target frequency of 4 Hz.

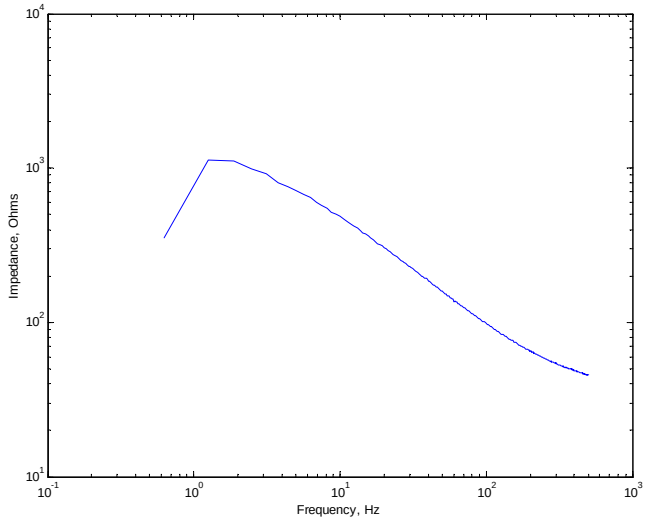

Figure 3.10: Impedance of the EM1 energy harvester device.

Impedances for the single samples are shown in Figure 3.11. There appears to be some scatter between the samples, especially at lower frequencies, but they all fall within the same range. The multilayer stack data shows a linear increase with increasing layers, Figure 3.12. This supports the theory that slipping of the layers causes the irregularities in the voltage and current stack data since strain does not factor into the impedance.

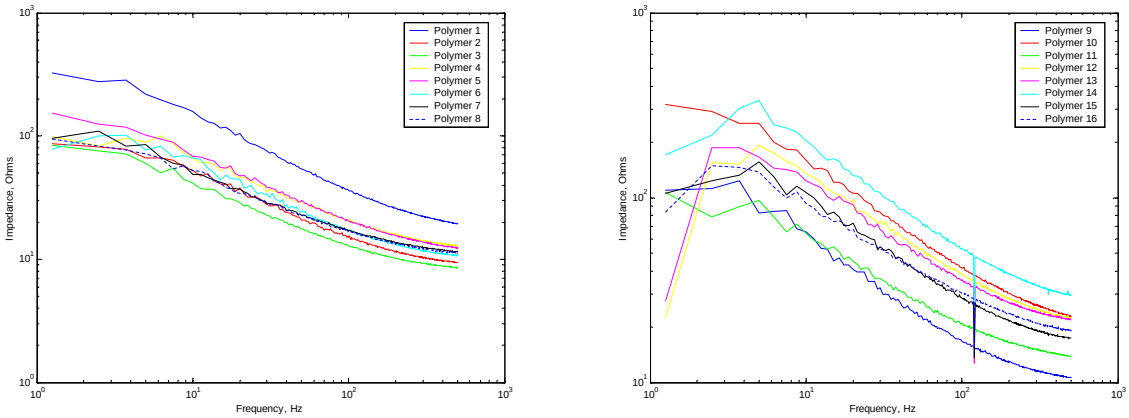

a) b)

Figure 3.11: Impedance for the single polymer samples.

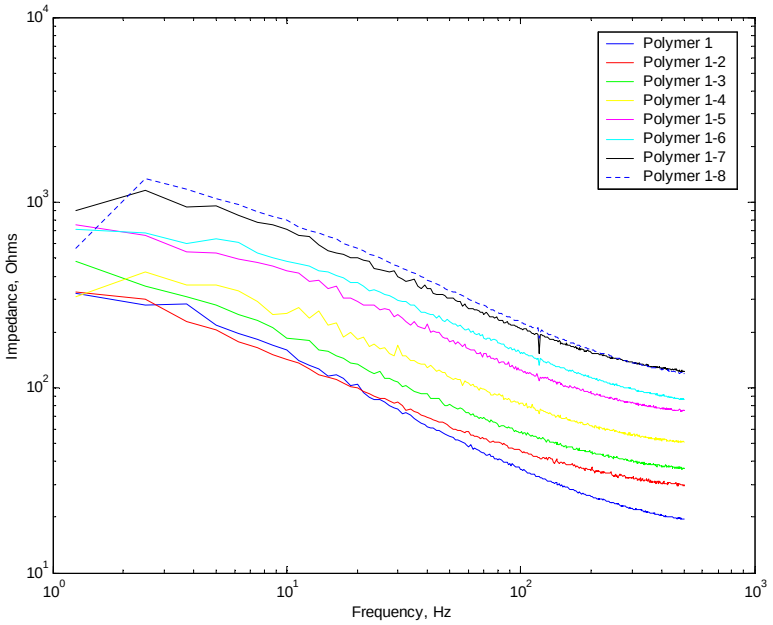

Figure 3.12: Impedance for the multilayer stacks showing a linear increase.

3.4 Power Calculations

Power is the product of voltage and current. Using the voltage transfer function and the current transfer function it is possible to calculate the power being produced by the ionic polymer energy harvester. However, simply multiplying the voltage and the current overestimates the power by a factor of four. Matching the impedance of the rectifier circuit, the load, to that of the transducer device, the source, doubles the resistance. This increased resistance reduces the amount of current and voltage by half. To correctly calculate the power that can be collected, the power transfer function must be divided by four,

$$P(\omega) = \frac{V(\omega)}{2}\frac{I(\omega)}{2} \tag{3.4}$$

as illustrated in Figure 3.13.

The calculated power transfer function is shown in Figure 3.14. The units of the power transfer function are μW/cm^2, but it is not power per area. Since both the voltage and current transfer functions are functions of deflection, this dependence becomes squared in the power transfer function. To correctly estimate the power produced by EM1 its deflection must be squared before being applied to the transfer function in Figure 3.14.

The expected power of EM1 can be calculated using the power transfer function and the expected deflection of ± 0.507 cm. At the target frequency of 4 Hz, EM1 produces 0.003 μW/cm^2. During one complete stroke the energy harvester will produce approximately 0.003 μW, a negligible amount of power. The low power is due to very low current being produced by the polymers, only a few microamps. While millivolts of voltage might be sufficient to harvest power, the low current makes it impossible to generate a significant amount. At the target operating frequencies the ionic polymers will not work as generators. However, at larger frequencies all of the transfer functions show much more mechanical energy being converted to electrical energy. It is possible that at these higher frequencies the ionic polymers could harvest usable power.

3.5 Examination of the Transfer Functions

In an effort to explain the shape of the transfer functions, two properties of the ionic polymers are analyzed: the natural frequencies and the impedance. By examining each of these properties an explanation for the shape of the transfer functions is clear.

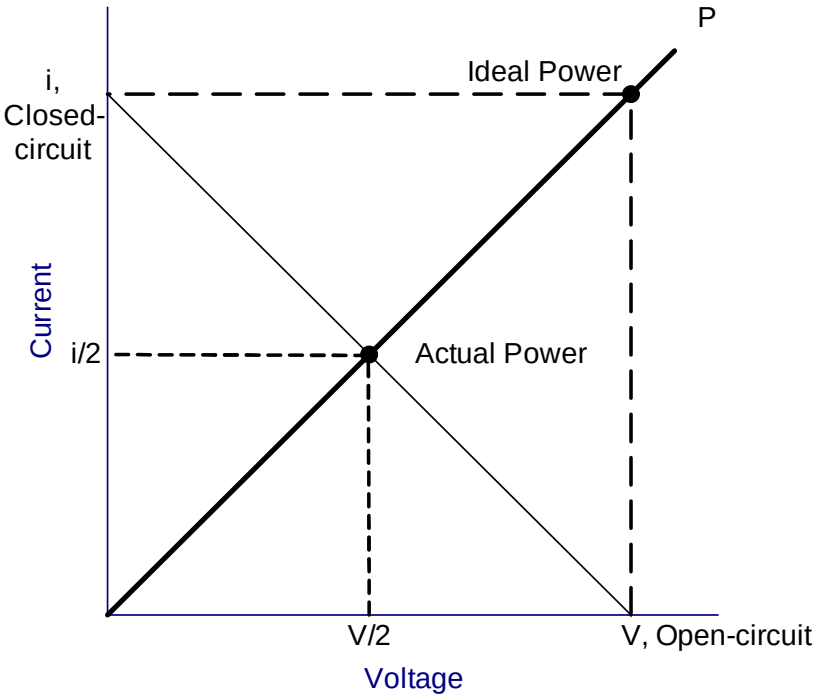

Figure 3.13: Power concept illustration.

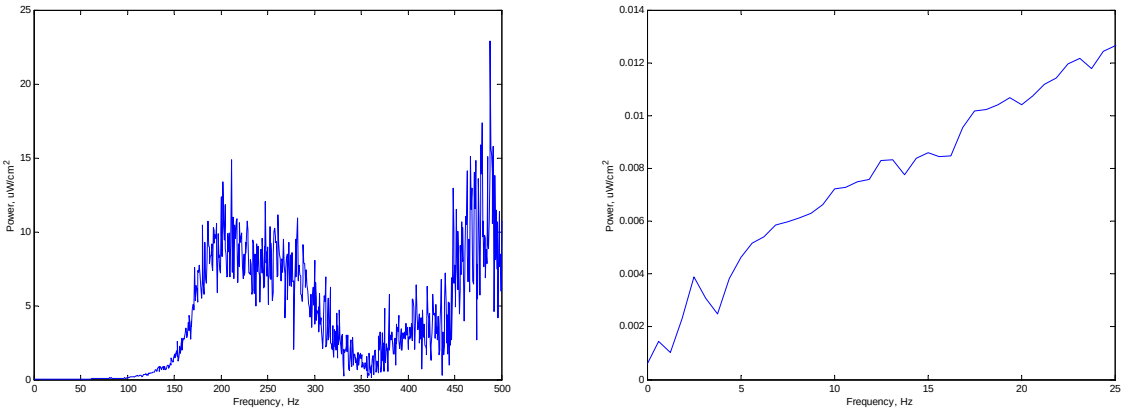

a) b)

Figure 3.14: Calculated power transfer function for the EM1 energy harvester: a) full bandwidth b) low frequencies.

3.5.1 Natural Frequency Analysis

The transfer functions show a large increase in electrical energy between 150 and 300 Hz, with a peak near 200 Hz. An analysis is performed on the ionic polymer posts to determine if a natural frequency exists at this point. The boundary conditions chosen for the analysis are clamped-sliding. Although one end of the polymers is completely unrestrained, the dual posts working in parallel cause the deflected shape to resemble the clamped-sliding boundary conditions. The mode shapes were calculated with the following equations for natural frequencies and mode shapes (Inman, 2001),

$$\omega_n = \beta_n^2 \sqrt{\frac{EI}{\rho A}} \tag{3.5}$$

$$\text{Mode Shapes} = \cosh(\beta_n x) - \cos(\beta_n x) - \sigma_n(\sinh(\beta_n x) - \sin(\beta_n x)). \tag{3.6}$$

The mode shapes and natural frequencies are calculated for both the fixed-free and fixed-sliding boundary conditions so the results could be compared. The first mode shapes for the two boundary conditions are compared in Figure 3.15. Comparing Figure 3.16 to the mode shapes of Figure 3.15 it is easy to see that clamped-sliding is a better choice for the boundary conditions.

The natural frequency calculations are performed for both the ionic polymer posts and the individual polymer samples. For the analysis the posts are assumed to be a solid beam with the following dimensions 2.35 cm $\times$ 1 cm $\times$ 0.16 cm. Dimensions for the individual samples were 2.35 cm $\times$ 1 cm $\times$ 0.02 cm. The first five natural frequencies for each case are shown in Table 3.1.

Table 3.1 makes it clear that the natural frequencies of the post are not the reason for the peak in the transfer functions, but that the natural frequencies of the individual polymers are responsible. The posts frequencies are high, most likely due to their short, wide geometry. The individual samples, which are thinner, have much lower frequencies. The calculations show that for both boundary conditions the first natural frequency of the individual sample is reasonably close to the peak in the transfer functions. The clamped-sliding boundary condition predicts a natural frequency of 181 Hz, which is precisely where the peak in the transfer functions appears. This evidence suggests that the individual polymer samples are being excited even though they are wrapped during testing.

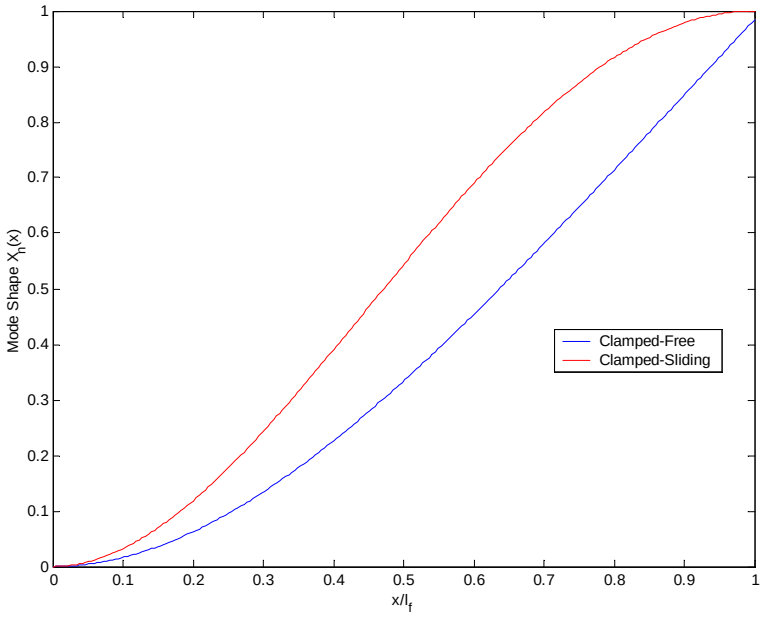

Figure 3.15: Mode shape comparison for the clamped-free and clamped-sliding boundary conditions.

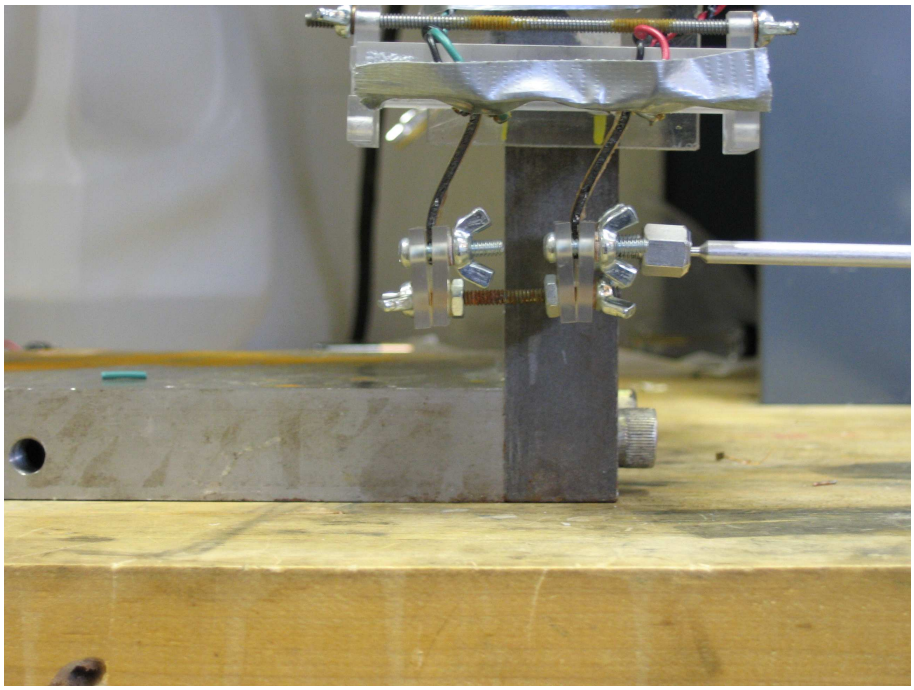

Figure 3.16: Shape of deflected EM1 model.

Table 3.1: Calculated natural frequencies of the posts and samples for clamped-free and clamped-sliding boundary conditions.

	Posts		Individual Samples	
Freq	Clamped-Free	Clamped-Sliding	Clamped-Free	Clamped-Sliding
f_1	1820	2895	114	181
f_2	11406	15646	713	978
f_3	31938	38637	1996	2415
f_4	62585	71845	3912	4490
f_5	103457	115272	6466	7205

3.5.2 Impedance affect on Power Generation

Understanding the definition of impedance, the ratio of voltage to current, makes it simple to explain why there is almost no current production by the polymers at low frequencies. Examining Figure 3.10 shows that the impedance at low frequencies is more than 600 Ohms, a voltage to current ratio of at least 600 to 1. The impedance of EM1 remains above 100 Ohms until the frequency reaches approximately 100 Hz. Around 100 Hz is also when the current production of the polymers increases. At low frequencies, <100 Hz, the impedance of EM1 is an order of magnitude greater than at higher frequencies. The impedance is too great to produce adequate current and hence adequate power.

3.6 Chapter Summary

Chapter 3 presented the power generation testing of the ionic polymer energy harvesting design. The model, denoted EM1, was placed in a test fixture that simulated the fixed-free boundary conditions of the proposed design. EM1 was then excited mechanically and the electrical power generation was measured. Transfer functions were obtained for the open-circuit voltage, closed-circuit current and impedance. Using the transfer functions the expected voltage and current were calculated for one complete stroke of the device at 4

Hz. The device produces 3.8 mV/cm, which for a stroke of ± 0.507 cm, is approximately 3.8 mV per stroke. The current production at the target frequency was 4.5 μA/cm, which is approximately 4.6 μA per stroke. The impedance of the device was 800 Ω. Individual samples and multilayer stacks of different sizes were also characterized for voltage, current, and impedance. Each single sample showed the same performance insuring that there are no damaged polymers. However, the voltage did not scale linearly with the layers. This error is due to the layers slipping and changing the strain from test to test. Current production from the multilayer stacks was relatively the same as expected for series stacking. The impedance did show a linear increase with added layers, confirming the theory that strain differences were the cause of the irregularities in the voltage data from the multilayer stacks. Power was calculated from the voltage and current transfer functions. The expected power at 4 Hz is 0.003 μW, a negligible amount of power. An analysis of the natural frequencies of the polymer samples and posts was performed to help explain the shape of the transfer functions. The individual polymer samples have a natural frequency at 181 Hz. The increased production of the device near this frequency is the result of the individual samples in the posts resonating. The next chapter presents the tests of the device as an energy storage vessel. Data on the charge and discharge characteristic of the design are discussed.

Chapter 4

Energy Storage

Power generation is not the only energy harvesting application of ionic polymers, energy storage is another possibility. Ionic polymers are highly capacitive. If another device is used to harvest the energy, the polymers could potentially replace a capacitor bank as a means of storing the energy. This use of the ionic polymers is intriguing for two reasons. First, the polymers are a new technology and their performance is likely to improve with further development. This means that while recent testing already shows promise for energy storage, this potential can be improved and optimized later. Second, the polymers can be manufactured into a myriad of shapes and dimensions. Conventional capacitors will be restricted to commercial sizes and shapes. Also, they will likely have to be wired to a circuit board. Both of these restrictions take up space inside the harvester device packaging where space is at a premium. The polymers can be manufactured in the desired shapes or dimensions to fit the needs of the harvester. They could be fitted around the harvester device and electronics, molded as a lining around the inside of the packaging, or even inserted as part of the packaging container. EM1 was tested to evaluate the energy storage potential of the proposed design. However, the configuration of polymers in the EM1 design is not the optimum configuration for storing energy. The two posts are in parallel, but the individual samples forming the posts are in series. Capacitors should be used in parallel so that the capacitance adds. Capacitors wired in series actually diminish the overall capacitance. However, testing the EM1 design will still provide an idea of the energy storage potential of the ionic polymers and highlight a few ways that the storage ability can be improved.

The ionic polymers are tested to determine how fast they will charge, the amount

of energy that can be stored, and how long the energy can be stored. During testing the design is observed while charging and also after the signal has been removed. A virtual instrument model is built in Simulink and linked to a ControlDesk real-time interface. The RTI allows the user to control dSPACE DAC and AD boards. Using this setup, a signal can be sent to the polymers to supply the charging current. Before the dSPACE signal is sent to the polymers it passes through a transconductance amplifier, which converts the controlled voltage signal to a controlled current signal. This allowed the polymers to be charged at a constant current level. The results of the testing, the capacitive characteristics of EM1, are examined in this chapter.

4.1 Charging with DC Current

A constant current signal is used first to charge the polymers. Using a step function, constant current is applied to the polymers for five minutes and then removed. The polymers are monitored for another ten minutes to observe any self-discharge. Charging of the polymers is done with input signals of various magnitudes.

Initial testing shows that the polymers charge extremely well. Once the current is applied, voltage rises sharply. However, after an initial rapid charging the polymers continue to acquire and store voltage at a decreasing rate. There appears to be a limit on the amount of voltage that can be stored with the maximum amount of voltage being dependent on the magnitude of the charging source. Once the stored energy reaches a constant voltage level the source is removed, which short-circuits the polymers. With no resistance except for that of the material there is a rapid self-discharge. The rate of the discharge then decreases, but does not reach zero in the test time frame. The initial rapid discharge is likely the result of electrolysis. The solvent in these particular ionic polymers is water, which requires only 1.23 V for electrolysis to occur. However, electrolysis is not entirely responsible for the self-discharge. When the stored voltage is above 1.23 V it does not always fall to that voltage during the initial discharge. Also, when the stored voltage is well below the electrolysis voltage there is still some discharge, although it is less severe. At the point where the charging rate goes to zero, the polymers are likely discharging energy at the same rate that it is being supplied. The charging tests are shown in Figure 4.1.

The two posts that comprise EM1 are charged separately to ensure that both are

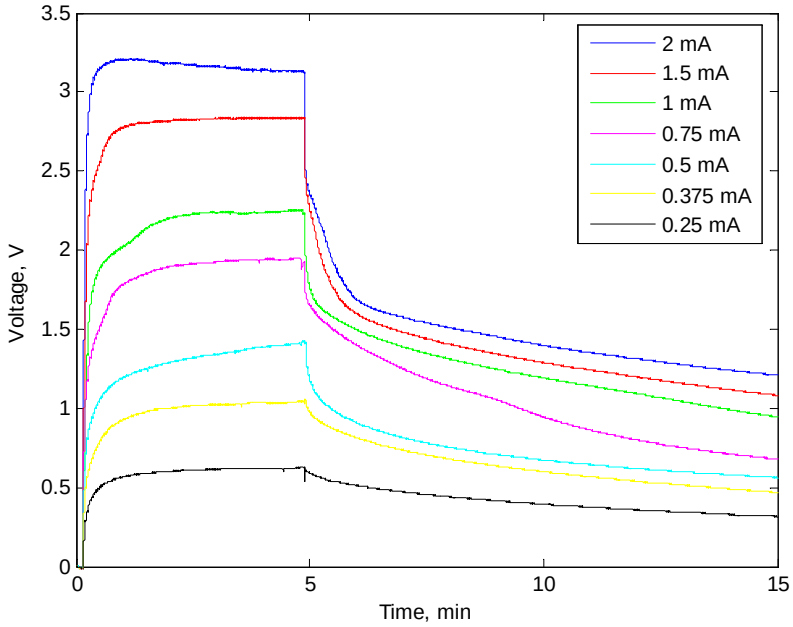

Figure 4.1: Charge and discharge characteristics of the ionic polymers at different input signal magnitudes.

functioning properly. This test also provides a means to check if increasing the amount of ionic polymers increases the capacitance. Each post is charged and allowed to discharge in the same fashion as the EM1 device. The results are compared in Figure 4.2 a) where the solid lines represent the left post and the dashed lines represent the right post. Both posts have similar charging and discharging paths. The left post (solid data lines) holds slightly higher voltages. It also shows more gradual discharge curves, but this can be attributed to small experimental variations. Essentially, both posts have similar performance characteristics, proving the ionic polymers are functioning properly in each post.

At first glance a single post appears to store approximately the same voltage, and have the same capacitance, as when both posts are used in parallel. However, examining a model of the ionic polymers will show that the capacitance and power is larger when both posts are used. A common model of ionic polymers is a resistor in series with a capacitor as in equation 4.1,

$$Z(j\omega) = Rp + \frac{1}{j\omega C_a} \tag{4.1}$$

where $Z(j\omega)$ is the complex impedance transfer function (Akle et al., 2004). Therefore,

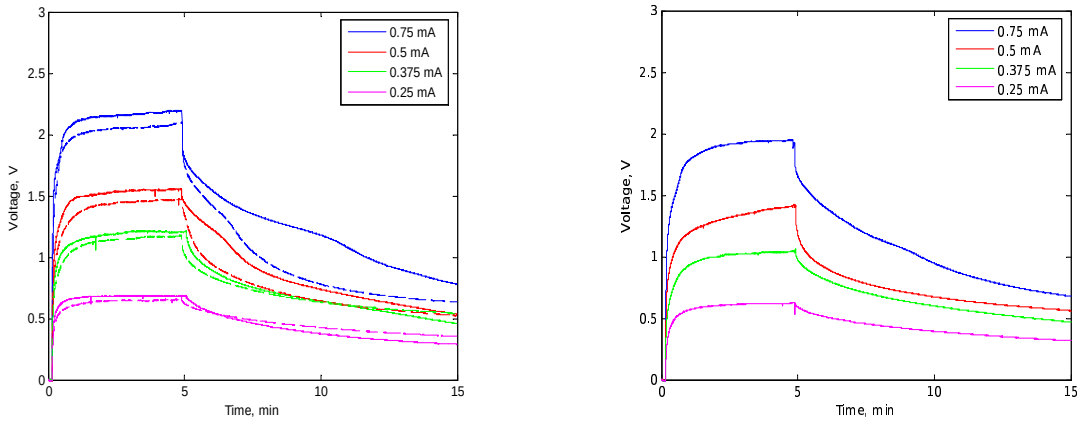

a) b)

Figure 4.2: Charge and discharge comparison of the individual posts and the EM1 device: a) Characteristics of the individual posts with the left post represented by a solid line and the right posts represented by a dashed line. b) Characteristics of the EM1 device.

since each post is constructed of eight identical polymer samples, each post has the same equivalent resistance and capacitance. Putting the posts in parallel causes two things to happen, the overall resistance is cut in half and the overall capacitance doubles. Capacitance is related to current with the following relationship (Hambley, 1997),

$$i = C_a \frac{dv}{dt} \tag{4.2}$$

which can explain the similar voltage curve between the single posts and the combined post device. When the two posts are placed in parallel the current is split between them, but the capacitance is doubled, so the rate of voltage being stored is equivalent. However, the power, as a function of capacitance and voltage as in equation 4.3,

$$P = vC \frac{dv}{dt} \tag{4.3}$$

increases since the voltage is constant but the capacitance is doubled. In the experimental setup, increasing the amount of polymers used for storage will not increase the voltage stored, but it will increase the amount of energy stored by increasing the overall capacitance.

Curves were fit to the data to estimate how long the ionic polymers will store energy before completely discharging. The data is first truncated so that only the discharge curve is used for the curve fit. The entire discharge curve resembles a power function, which is used as the first model. The equation for the power function model is,

$$y_p = 1.6296 x_{fit}^{-0.14792}. \tag{4.4}$$

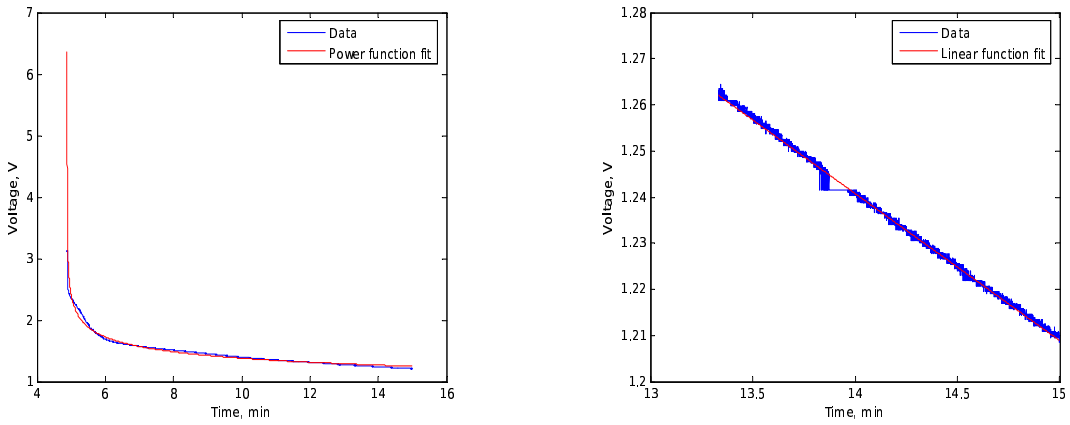

a) b)

Figure 4.3: Models fit to the data: a) Power function model of entire discharge curve. b) Linear function model of linear portion of discharge curve.

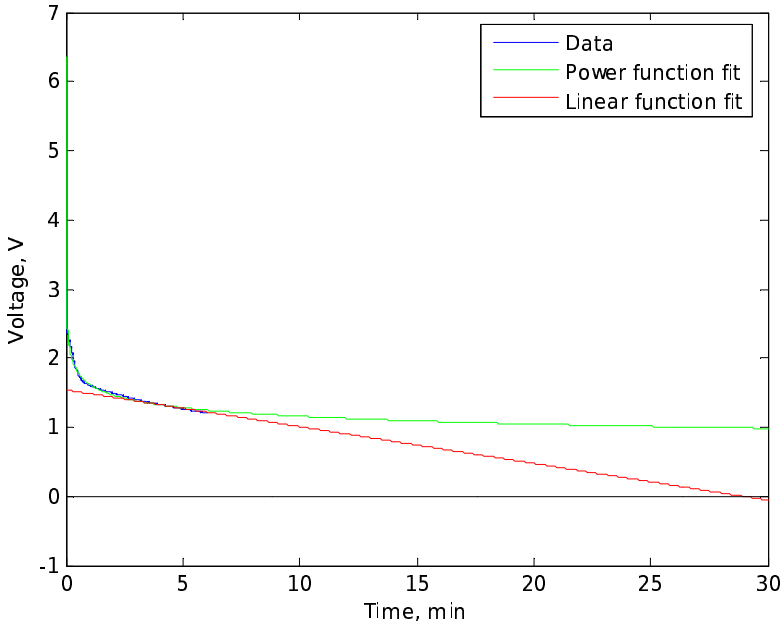

Figure 4.4: Comparison of both models to the discharge data. The time scale is shifted to show only the time after discharge begins.

However, the power function model approaches an asymptote near the end of the data window while the polymers continue to discharge slowly. To provide a better fit near the end of the data, it is again truncated until only the data with an almost linear slope remains. A linear fit is then calculated for the data producing the following equation,

$$y_l = -0.05317x_{fit} + 1.2621. \tag{4.5}$$

The two fits provide a best and worst case scenario with the actual discharge of the polymers somewhere in the middle. While the current polymers will probably never completely hold charge like the power function model the discharge is not as drastic as the linear model. The power fit and linear fit are shown in Figure 4.3. The comparisons of both fits and the data are shown in Figure 4.4. Based on the fits and the data, the polymers can store energy for several hours before completely discharging.

4.2 Charging with AC Current

Charge and discharge testing is also performed on the ionic polymers using an AC current signal. Several different frequencies of a 1 mA AC current signal are used to charge the EM1 device. An AC signal is representative of the raw signal that an energy harvester would generate from oscillating vibrations. If the polymers can be charged with an AC signal it would eliminate the need for a rectifier circuit between the harvesting device and the polymer capacitor bank.

AC testing is performed with low frequencies since the operating frequencies are between 0.2 and 4.2 Hz. Even with these low frequencies the polymers do not charge well with a alternating source. The voltage in the polymers is constantly driven by the source and very little voltage is actually stored in the polymers. As the frequency of the AC signal is lowered there is a slight improvement in the voltage storage. The lower frequency signal allows the polymers to charge to a higher absolute voltage, but the net voltage stored remains the same. To be able to store large amounts of energy a rectifier circuit is needed to convert the AC signal to DC. The results of the AC charging tests are shown in Figure 4.5.

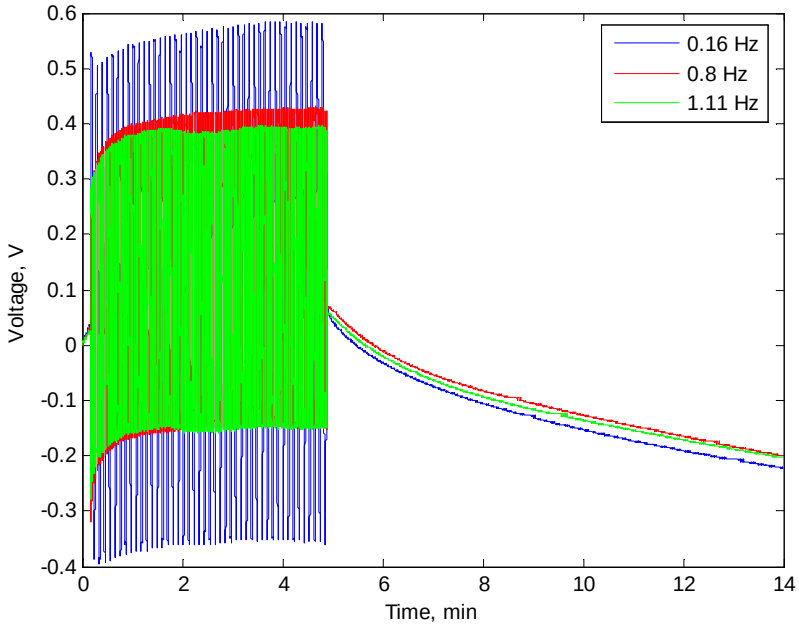

Figure 4.5: Charge and discharge characteristics of the ionic polymers using an AC charging signal. Frequencies of the signal are varied but the magnitude is a constant 1 mA.

4.3 Comparison of Ionic Polymers to an Equivalent Capacitor

A comparison is performed between ionic polymers and commercial electrolytic capacitors to gauge the performance of the polymers as capacitors. The capacitance of EM1 can be calculated from the impedance transfer function. Using the imaginary component of equation 4.1,

$$C_a = \frac{10^3}{Im(Z(j\omega)) \times \omega} \tag{4.6}$$

the capacitance of the EM1 device is computed in millifarads for the frequency bandwidth. The DC capacitance, 0.82 mF, is used for the equivalent capacitance of the commercial capacitors since EM1 is charged with a DC signal. The calculated capacitance of EM1 is shown in Figure 4.6.

Using standard electrolytic capacitors, an equivalent capacitance is tested and observed to compare with the charge and discharge characteristics of the EM1 device. A resistance is placed in series with the equivalent capacitance since the polymers also have an inherent resistance. The DC resistance of the EM1 is approximately 200 Ω. Comparisons

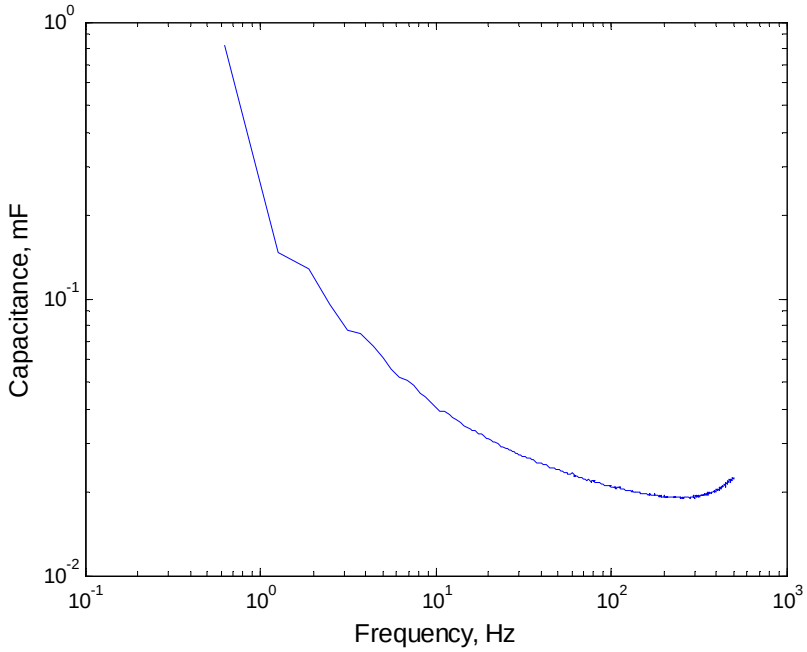

Figure 4.6: Capacitance of the EM1 energy harvesting model.

of the EM1 device and an equivalent capacitance are shown in Figure 4.7. The commercial capacitors outperform the ionic polymers in the amount of energy they can store and the rate of discharge. Commercial capacitors are able to achieve higher voltages per milliamp of current sent to the capacitor. Also, commercial capacitors have a slower discharge rate once the charging source is removed. However, both the capacitance and the discharge rate has the potential to be improved in the ionic polymers. Using an ionic liquid as a solvent will improve the degradation voltage of the polymers, thus improving the capacitance at higher voltages. Increasing the thickness of the polymers will improve the resistance, which will slow the discharge rate. After the initial rapid discharge the ionic polymers hold a voltage very well. The long term rate of discharge is comparable to the electrolytic capacitors.

Another difference between the ionic polymers and the electrolytic capacitors is the storage ability at higher charging currents. The capacitance of the commercial capacitors remains approximately constant with changing current levels. Plotting voltage per current, as in Figure 4.8, the ionic polymers show a decreasing amount of capacitance as the charging current is increased. This is likely a result of the electrolysis occurring in the ionic polymers. As higher voltage levels are reached, the rate of electrolysis increases diminishing the capacitance. Again, using a different solvent could improve storage ability.

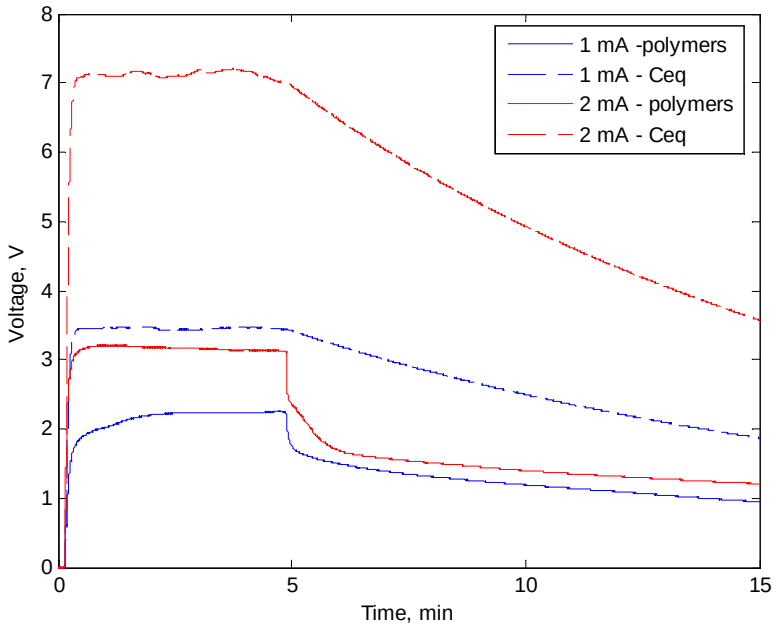

Figure 4.7: Comparison of EM1 capacitance to an equivalent electrolytic capacitance.

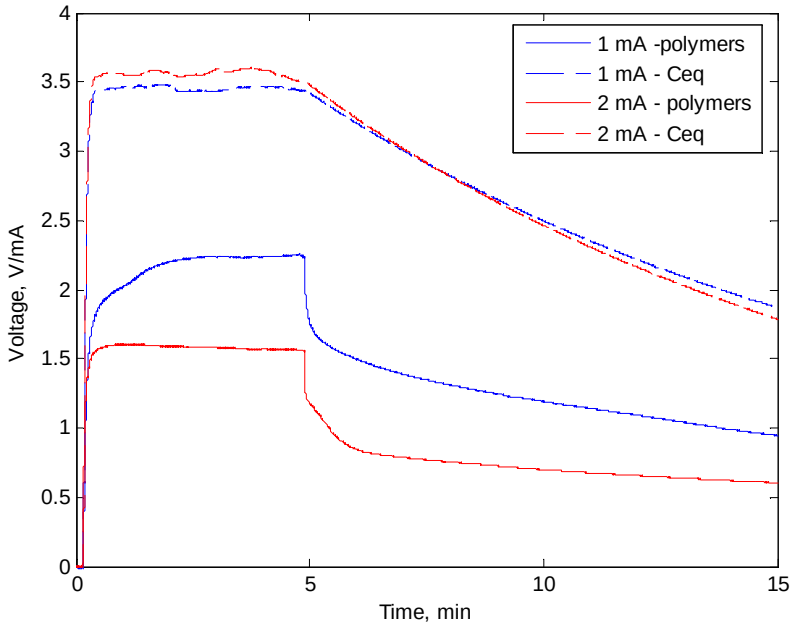

Figure 4.8: Voltage per current comparison of EM1 and an equivalent electrolytic capacitance.

4.4 Discharging across a Load

The ionic polymers are discharged across varying loads to calculate the amount of power stored. Resistors, ranging from 10 Ω to 1 kΩ, are placed in series with the EM1 device to act as a load. Using dSPACE the polymers are charged to 1 V. When that voltage is reached the charging signal is removed and the current is measured with a multimeter. Measurements were taken every minute for fifteen minutes. The current measured is presented in Figure 4.9. The initial rapid discharge seen in Figures 4.1 and 4.2 occurs in the first minute and is not recorded. The recorded data shows a gradual decrease in current during the first five minutes and then an almost steady current for the remaining ten minutes. The same behavior is seen in the voltage figures and shows how well the polymers can store energy over time. The magnitude of the current declines as the resistance of the load is increased, the expected result since the peak voltage is fixed.

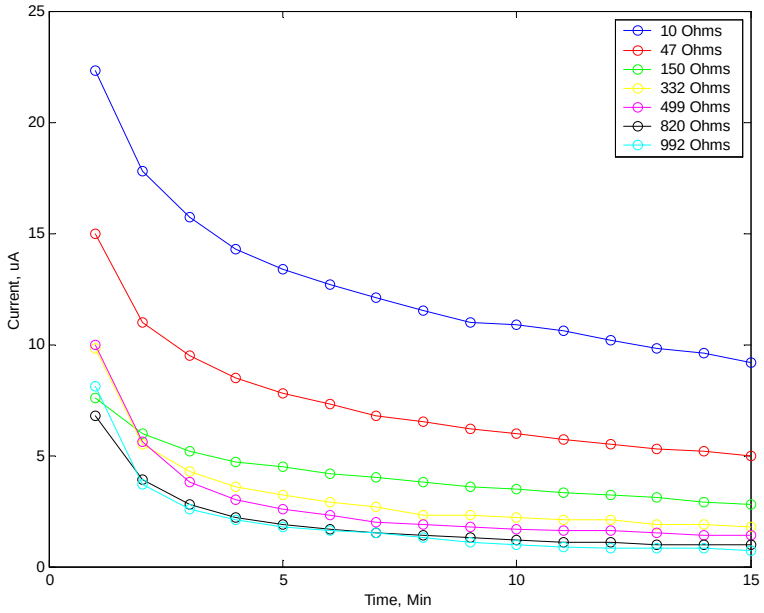

Figure 4.9: Stored current in the EM1 device discharged across varying loads.

Discharging the ionic polymers across a load made it convenient to calculate the available power. Substituting for v in Ohm's Law, power is calculated from the current and the resistive load (Hambley, 1997),

$$P = Ri^2. \tag{4.7}$$

The power is shown in Figure 4.10. The stored power is in the same range as the generated power, only a few nanowatts. Low current is the limiting factor for the stored power as it was for the power generation. However, this limitation might be improved by configuring the polymers in parallel which would maximize the capacitance. Looking at the lower portion of the current range, as shown in Figure 4.11, the power is maximized with a resistive load of 150 Ω. The power is maximized because that resistance matches the impedance of the EM1 device. This match is verified by Figure 3.10, which is approximately 300 Ω at 0.6 Hz. Extended the curve toward 0 Hz would likely put the impedance in the range of 150 Ω.

4.5 Chapter Summary

This chapter presented the results of the energy storage testing. Constant current signals of varying amplitudes were used to charge the EM1 device. The stored voltage was measured during charging and discharging. The polymers charge extremely well, however, performance deteriorates when higher voltages are achieved. For example, when charging the polymers with 1 mA the peak voltage reaches 2 V, but when charging with 2 mA the peak voltage is approximately 3.25 V. An attempt was made to charge the polymers with an alternating current, but this was not successful. The alternating current constantly drove the amount of voltage in the polymers and the net effect was that very little energy was stored. The capacitance of EM1 was calculated from the impedance. The DC capacitance of the polymer device is approximately 0.82 mF. An equivalent capacitance was constructed from standard electrolytic capacitors to be compared with the ionic polymers. The commercial capacitors are able to store more energy than the polymers, but the long term storage ability is comparable. Current was measured across resistive loads ranging from 10 to 1000 Ω. The power was calculated and found to be on the same order, nanowatts, as the power generated. Power was maximized for a resistive load of 150 Ω. The conclusions of the research are presented in the following chapter.

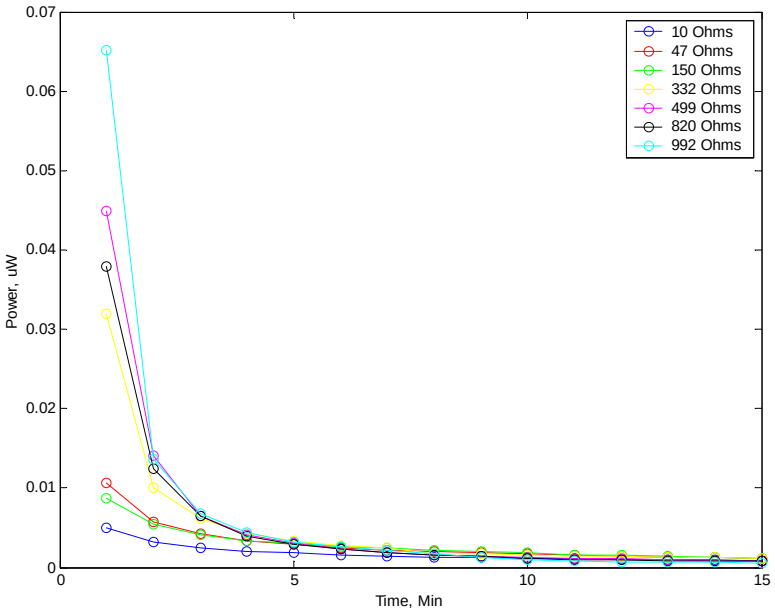

Figure 4.10: Power stored by the EM1 device for various loads.

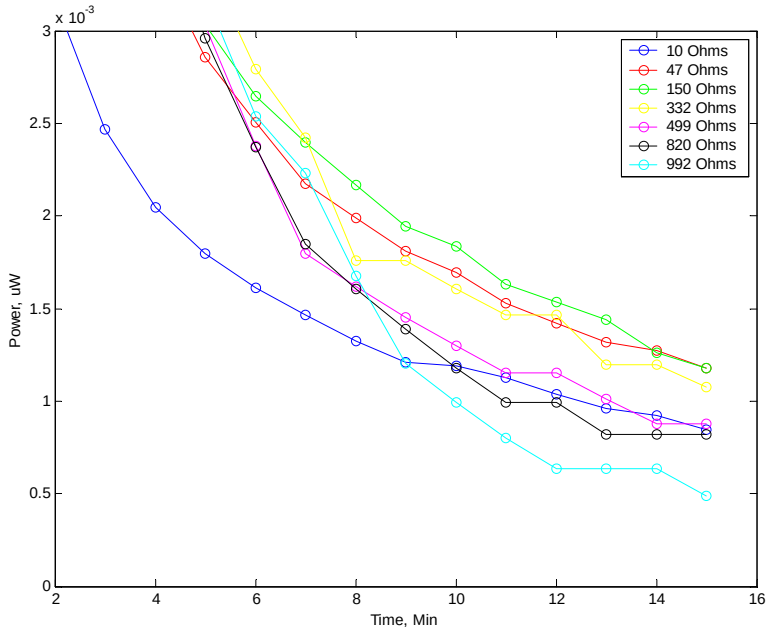

Figure 4.11: Power is maximized by the 150 Ω load.

Chapter 5

Conclusions

The work presented in this thesis focused on finding unique applications for ionic polymers as energy harvesters. The specific need that drove the research is a self-contained wireless sensor powered by harvested energy from ambient vibrations. Locating a renewable power source with a sensor will enable the sensor unit to be wireless and require minimal maintenance. Ionic polymers were explored as energy transducers and as agents for energy storage. An ionic polymer device was designed to fit the need and tested to determine whether it is a viable option for harvesting or storing energy. This chapter restates the contributions of the work and presents the conclusions of the research. Also, future work for exploring and quantifying ionic polymers for energy harvesting applications is discussed.

5.1 Contribution

The research presented in this thesis is the development and analysis of applications for ionic polymers as energy harvesting devices. The specific application for mounting the energy harvesting device on ship propulsors incorporated strict environmental guidelines including the the frequency of the vibrations, loading magnitudes, and dimensions. Using the design requirements, design curves were generated to develop an ionic polymer device that could function as an energy harvester in the described environment. The selected design was then characterized to determine the amounts of electrical energy that could be harvested by mechanically exciting the device. Transfer functions were collected to quantify the open-circuit voltage and closed-circuit current. Data was collected for frequencies up to 500 Hz. The impedance of the device was also measured for the same bandwidth. The

expected power that the ionic polymer device could produce was calculated using the voltage and current. The power calculation included adjusting for the increased resistance from matching the impedance of the polymer device to the required rectifier circuit. Therefore, the power calculated is the actual power expected after the raw AC signal has been converted to a DC supply. Ionic polymers were also considered as the energy storage vessel for the harvesting application. The capacitive characteristics of the design were investigated for the purpose of using the polymers in place of a standard capacitor bank. The ionic polymer device was tested to determine the charge and discharge characteristics, which were then compared to commercial capacitors.

5.2 Research Conclusions

An energy harvesting device can be designed to use ionic polymer materials.

A two-post ionic polymer design that will fit inside the prescribed environment is presented in Chapter 2. The design provides dimensions for the polymer material as well as the head mass needed to provide the strain. The device is tuned to a frequency of 7 Hz, very close to the operational range of 0.2 to 4.2 Hz. It was tuned to a frequency outside the operational range to avoid resonance. Under the estimated loading the polymer device can survive the axial and lateral stresses incurred during operation, calculated to be 25 MPa and 22 MPa respectively. However, it does not have a factor of safety as stresses are barely below the allowable limit. Since both the axial and lateral stresses are close to the failure limit the combined axial stress is above the allowable stress of the material. Also, the ionic polymers buckle under the static weight of the head mass. Critical buckling stress is calculated to be 0.387 kg, but testing shows that the design can only support 0.23 kg. Both values are significantly smaller than the design mass of 0.816 kg.

The design can be modified in a number of ways and still function as an energy harvester. One reason the design was tuned to 7 Hz was to avoid resonance effects that would amplify deflections. Another was the thought that given the loading and space constraints, tuning the design to 4 Hz would be impossible. In hindsight, 7 Hz was also too low. Increasing the tuning frequency would increase the stiffness of the polymer posts and decrease the stresses. Testing would need to be performed to insure that the device would still be excited by the operating frequencies if the tuning frequency was increased. Another

option for reducing the stress is to reduce the initial target strain. All design calculations were based around 10% axial strain. However, lowering the target strain would reduce the amount of converted energy. Another option would be to support the headmass with a different material becuase the ionic polymers cannot support much weight staticlly . Using a support post, with equivalent stiffness, but made from a material with larger allowable stress would solve both the stress and buckling issues. The ionic polymers could still be strained laterally, but not have to support any loading axially.

At the low frequencies targeted for this study, the current ionic polymer transducers cannot produce usable power as energy harvesters.

The energy production of the design was characterized as explained in Chapter 3. Open-circuit voltage, closed-circuit current, and impedance were quantified for a bandwidth of 500 Hz. The ionic polymer device produces decent voltage, between a few millivolts per centimeter at low frequencies and 100 millivolts near the end of the bandwidth. At the highest estimated operating frequency, 4 Hz, the device produces approximately 3.8 mV/cm. At the peak of current production the device produces approximately 1 mA/cm. However most of the current data is in the range of microamps per centimeter. Approximately 4.5 uA/cm of current is produced at the operating frequency. The impedance of ionic polymers decreases with increasing frequency. The impedance of the harvester device shows an initial increase at low frequencies but then declines. The largest impedance is approximately 1000 Ω and the lowest approximately 45 Ω. At 4 Hz the impedance is 800 Ω. Expected power was calculated from the open-circuit voltage and the closed-circuit current. To maximize the power of the harvested energy, the impedance of the device and the rectifier circuit need to be matched. Doubling the resistance reduces both the voltage and current by half. Therefore, the expected power produced by the ionic polymer device is 0.003 $\mu W/cm^2$ at 4 Hz. The extremely low current produced at low frequencies is the biggest limiting factor in energy production. Large impedances at these frequencies limit the amount of current. The result is that the ionic polymers cannot generated enough power to be used as a renewable supply at low frequencies.

The ionic polymers do show potential as energy storage vessels.

The same energy harvesting device tested for energy generation was tested for energy storage, which is discussed in chapter 4. Both the charging and discharging characteristics of the polymer device were recorded. The polymers were charged with a constant current signal while the voltage accumulating was monitored. The polymers charge extremely well, however, performance deteriorates when higher voltages are achieved. For example, when charging the polymers with 1 mA the peak voltage reaches 2 V, but when charging with 2 mA the peak voltage is approximately 3.25 V. The nonlinearity in peak voltage is likely the result of electrolysis occurring and using some of the stored energy. An attempt was made to charge the polymers with an alternating current, but this was not successful. The alternating current constantly drove the amount of voltage in the polymers and the net effect was that very little was stored. An energy storage comparison was performed between the ionic polymers and commercial capacitors. The capacitance of the polymer device was calculated from the impedance and an equivalent capacitance was tested. The DC capacitance of the polymer device is approximately 0.82 mF. The electrolytic capacitors outperformed the ionic polymers by achieving higher voltages per milliamp of charging current. Also, the performance of the capacitors is unaffected by higher voltages, doubling the charging current doubled the peak voltage. The polymers did have comparable discharge characteristics. There is an initial rapid discharge of the polymers, but once that is over they hold a voltage well over time. Current was measured across resistive loads ranging from 10 to 1000 Ω. The power was calculated and found to be on the same order, nanowatts, as the power generated. Although the power is small, the ionic polymers are able to discharge energy across a load proving that they are capable of supplying power.

5.3 Recommendations for Future Work

Based on power generation characteristics of the ionic polymers future work in this area seems unneeded at this time. While the open-circuit voltage produced is decent, there is little current. With the current ionic polymers, producing a usable amount of power at low frequencies is not possible. However, power improves at higher frequencies, so if the operating frequency increases power generation could be a possibility.

The results of the energy storage tests do warrant further research. It was shown

that the ionic polymers have potential to be an agent for energy storage. However, only one type of ionic polymer and one configuration was tested. Future work should explore polymers with solvents other than water to try and decrease the effects of electrolysis on the stored energy. Also, the configuration of the polymers, stacked in series, was not ideal for maximizing the capacitance. Parallel stacking would increase the capacitance of multilayer stacks. Another area of exploration would be the dimensions of the polymer samples. Effort should be made to determine how surface area and thickness of the polymer samples effects the capacitance of the ionic polymers.

Bibliography

Akle, B. J., Hickner, M. A., Leo, D. J., and McGrath, J. E., *Correlation of Capacitance and Actuation in Ionomeric Polymer Transducers*, **Journal of Material Science**, 2004.

Anonymous, *Energy Scavenging*, **Noise and Vibrations Worldwide**, Vol. 34, No. 10, pp. 7–9, 2003.

Bar-Cohen, Y., **Electroactive Polymer (EAP) Actuators as Artificial Muscles - Reality, Potential, and Challenges**, SPIE Press, Bellingham, WA, 2001.

Beer, F. P. and E. R. Johnston, J., **Mechanics of Materials**, Second Edition, McGraw-Hill, 1992.

Blevins, R. D., **Formulas for Natural Frequency and Mode Shape**, Reprint Edition, Krieger Publishing Company, Malabar, Florida, 2001.

Chandrakasan, A., Amirtharajah, R., Cho, S. H., Goodman, J., Konduri, G., Kulik, J., Rabiner, W., and Wang, A., *Design Considerations for Distributed Microsensor Systems*, **Proceedings of the 21st IEEE Annual Custom Integrated Circuits Conference**, pp. 279–286, 1999.

Duffy, M. and Carroll, D., *Electromagnetic Generators for Power Harvesting*, **PESC Record - IEEE Annual Power Electronics Specialists Conference 2004 IEEE 35th Annual Power Electronics Specialists Conference, PESC04**, Vol. 3, pp. 2075–2081, 2004.

DuPont^{TM}, 2004, "Nafion® PFSA Membranes Product Information," Webpage, Http://www.dupont.com/fuelcells/pdf/nae101.pdf.

Gonzalez, A. M., De Frutos, J., Duro, C., Alemany, C., and Pardo, L., *Changes in the piezoelectric parameters of PZT ceramics during the poling process*, **Ferroelectrics**, Vol. 208/209, No. 1/4,1/2, pp. 449–457, 1998.

Hambley, A. R., **Electrical Engineering Principles & Applications**, Prentice Hall, Upper Saddle River, NJ, 1997.

Inman, D. J., **Engineering Vibration**, Second Edition, Prentice Hall, Upper Saddle River, NJ, 2001.

Keawboonchuay, C. and Engel, T., *Scaling Relationships and Maximum Peak Power Generation in a Piezoelectric Pulse Generator*, **IEEE Transactions on Plasma Science**, Vol. 32, No. 51, pp. 1879–1885, 2004.

Leo, D. J., 2003, "Active Materials and Smart Structures - I," Course Notes, Virginia Tech course ME 5984.

Mischke, C. R. and Shigley, J. E., **Mechanical Engineering Design**, Sixth Edition, McGraw-Hill, New York, NY, 2001.

Newbury, K. M. and Leo, D. J., *Electromechanical Modeling and Characterization of Ionic Polymer Benders*, **Journal of Intelligent Materials Systems and Structures**, Vol. 13, No. 1, pp. 51–60, 2002.

Newbury, K. M. and Leo, D. J., *Linear Electromechanical Model of Ionic Polymer Transducers - Part I: Model Development*, **Journal of Intelligent Materials Systems and Structures**, Vol. 14, No. 6, pp. 333–342, 2003a.

Newbury, K. M. and Leo, D. J., *Linear Electromechanical Model of Ionic Polymer Transducers - Part II: Experimental Validation*, **Journal of Intelligent Materials Systems and Structures**, Vol. 14, No. 6, pp. 343–358, 2003b.

Piezo Systems, I., 2005, Webpage, Http://www.piezo.com//.

Poulin, G., Sarraute, E., and Costa, F., *Generation of Electrical Energy for Portable Devices: Comparative Study of an Electromagnetic and a Piezoelectric System*, **Sensors & Actuators A-Physical**, Vol. 116, No. 3, pp. 461–471, 2004.

Roundy, S., Wright, P. K., and Rabaey, J., *A Study of Low Level Vibrations as a Power Source for Wireless Sensor Nodes*, **Computer Communications**, Vol. 26, No. 11, pp. 1131–1144, 2003.

Shahinpoor, M. and Kim, K. J., *Ionic polymer-metal composites: I. Fundamentals*, **Smart Materials & Structures**, Vol. 10, No. 4, pp. 819–833, 2001.

Shahinpoor, M. and Kim, K. J., *Ionic polymer-metal composites: II. Manufacturing Techniques*, **Smart Materials & Structures**, Vol. 12, No. 1, pp. 65–79, 2003.

Shahinpoor, M. and Kim, K. J., *Ionic polymer-metal composites: IV. Industrial and Medical Applications*, **Smart Materials & Structures**, Vol. 12, No. 1, pp. 197–214, 2005.

Sodano, H. A., 2003, **Macro-Fiber Composites for Sensing, Actuation and Power Generation**, M.S. Thesis, Virginia Polytechnic Institute and State University.

Sodano, H. A., Inman, D. J., and Park, G., *A review of Power Harvesting from Vibration using Piezoelectric Materials*, **Shock & Vibration Digest**, Vol. 36, No. 3, pp. 197–205, 2004.

Vita

Benjamin R. Martin was born on June 16, 1981 to Larry and Gail Martin of Harrisonburg Virginia. He began his college career at Virginia Tech in 1999 studying engineering. During summer breaks as an undergrad he worked as an intern for Flow Science, Inc. He graduated from Virgina Tech with a degree in mechanical engineering in May of 2003 and was accepted to graduate school for the fall of 2003. In January 2004 he began his Master's research for Dr. Don Leo at the Center for Intelligent Material Systems and Structures in the mechanical engineering department of Virgina Tech.

Address: Center for Intelligent Material Systems and Structures
310 Durham Hall
Blacksburg, VA 24061

This thesis was typeset with LaTeX 2_ε[1] by the author.

[1] LaTeX 2_ε is an extension of LaTeX. LaTeX is a collection of macros for TeX. TeX is a trademark of the American Mathematical Society. The macros used in formatting this thesis were written by Greg Walker, Department of Mechanical Engineering, Virginia Tech.